Protist, Vol. 162, 590–615, October 2011
http://www.elsevier.de/protis
Published online date 28 May 2011

Protist

ORIGINAL PAPER

Ultrastructure and LSU rDNA-based Phylogeny of *Peridinium lomnickii* and Description of *Chimonodinium* gen. nov. (Dinophyceae)

Sandra C. Craveiro[a], António J. Calado[a,1], Niels Daugbjerg[b], Gert Hansen[b], and Øjvind Moestrup[b]

[a]GeoBioSciences, GeoTechnologies and GeoEngineering (GeoBioTec) Research Unit and Department of Biology, University of Aveiro, P-3810-193 Aveiro, Portugal
[b]Section for Evolution and Ecology of Aquatic Organisms, Department of Biology, University of Copenhagen, Øster Farimagsgade 2D, DK-1353 Copenhagen K, Denmark

Submitted August 26, 2010; Accepted March 13, 2011
Monitoring Editor: Marina Montresor.

Several populations of *Peridinium lomnickii* were examined by SEM and serial section TEM. Comparison with typical *Peridinium*, *Peridiniopsis*, *Palatinus* and *Scrippsiella* species revealed significant structural differences, congruent with phylogenetic hypotheses derived from partial LSU rDNA sequences. *Chimonodinium* gen. nov. is described as a new genus of peridinioids, characterized by the Kofoidian plate formula Po, cp, x, 4′, 3a, 7″, 6c, 5 s, 5‴, 2⁗, the absence of pyrenoids, the presence of a microtubular basket with four or five overlapping rows of microtubules associated with a small peduncle, a pusular system with well-defined pusular tubes connected to the flagellar canals, and the production of non-calcareous cysts. Serial section examination of *Scrippsiella trochoidea*, here taken to represent typical *Scrippsiella* characters, revealed no peduncle and no associated microtubular strands. The molecular phylogeny placed *C. lomnickii* comb. nov. as a sister group to a clade composed of *Thoracosphaera* and the pfiesteriaceans. Whereas the lack of information on fine structure of the swimming stage

[1]Corresponding author; fax + 351 234372587
e-mail acalado@ua.pt (A.J. Calado).

Abbreviations: apc, apical pore complex; as, anterior sulcal plate; Ch, chloroplast; cp, cover plate; d, dictyosomes; E, eyespot; EV, elongated vesicle; f, fibre; LB, longitudinal basal body; LC, layered connective; LF, longitudinal flagellum; LFC, longitudinal flagellar canal; LMR, longitudinal microtubular root; ls, left sulcal plate; LSC, longitudinal striated collar; mt, mitochondria; N, nucleus; o, oil droplets; P, pyrenoid; pl, platelets; Po, pore plate; ps, posterior sulcal plate; PSC, peduncle striated collar; rs, right sulcal plate; SCc, striated collar connective; SMR, single microtubular root; T, trichocyst; TB, transverse basal body; TF, transverse flagellum; TFC, transverse flagellar canal; TMR, transverse microtubular root; TMRE, transverse microtubular root extension; TSC, transverse striated collar; TSR, transverse striated root; TSRM, transverse striated root microtubule; x, canal plate.

doi:10.1016/j.protis.2011.03.003

of *Thoracosphaera* leaves its affinities unexplained, *C. lomnickii* shares with the pfiesteriaceans the presence of a microtubular basket and the unusual connection between two plates on the left side of the sulcus, involving extra-cytoplasmic fibres.

Key words: *Chimonodinium*; Dinophyceae; LSU rDNA; *Peridinium lomnickii*; phylogeny; *Scrippsiella trochoidea*; ultrastructure.

Introduction

Peridinium lomnickii Wołoszyńska was originally described from ponds in the southeastern Polish region of Lwów (called Lemberg in the original German text), now Lviv, southwest Ukraine (Wołoszyńska 1916). The original description included mention of numerous chloroplasts and a central, oval nucleus. The report on the tabulation, combined with five drawings of the theca showing all major and some of the furrow plates, allow unambiguous identification of the species (Wołoszyńska 1916). A distinct preference for the winter period was noted for *P. lomnickii*, which attained its maximum development and formed blooms during the colder months (Wołoszyńska 1916, pp 264, 268).

Peridinium lomnickii has been reported from Europe, North America, South America, Tasmania, Japan and China (Eddy 1930; Lefèvre 1932; Lewis and Dodge 2002; Ling et al. 1989; Liu et al. 2008; Senzaki and Horiguchi 1994; Thomasson 1963). It was found abundantly in samples from shallow ponds shortly after thaw (Lindemann 1920, 1924) and was reported to occur mainly in cold waters with low organic content (Grigorszky et al. 2003b).

The current classification of *Peridinium* Ehrenberg, based on features of the theca, holds together species with and without an apical pore complex and with varying numbers of plates in epithecal and cingular Kofoidian series, while excluding species with a number of anterior intercalary plates smaller than two (Bourrelly 1970; Popovský and Pfiester 1990; Starmach 1974). The bulk of the excluded species possess an apical pore complex and are grouped in *Peridiniopsis* Lemmermann (Popovský and Pfiester 1990). Although plate arrangement in the furrows has been little used in the taxonomic organization of recent freshwater dinoflagellate floras (e.g. Lewis and Dodge 2002) the furrows are generally regarded as more conservative than other areas of the theca and formed the basis for the segregation of several marine genera (for a brief summary of the use in taxonomy of cingular plate number see Balech 1980; Bourrelly 1968; Indelicato and Loeblich 1986). The type species of *Peridinium*, *P. cinctum* (OF Müller) Ehrenberg, with five cingular plates and no apical pore, may therefore be more distantly related to *P. lomnickii* and other species of *Peridinium* and *Peridiniopsis* with six cingular plates and an apical pore than these species are among themselves. The ordering of *Peridinium* species into several distantly related groups in phylogenetic hypotheses based on SSU and LSU rDNA analyses (Logares et al. 2007) likewise suggests the need for revising generic boundaries within the peridinioids if a taxonomy reflecting phylogeny is to be achieved. This should preferably be based on the combination of external morphology, internal fine structure and DNA-derived phylogenies of representatives of various peridinioid groups.

For decisions to be made concerning the taxonomic position of *P. lomnickii* its features must be compared in detail with the typical features of closely related peridinioid genera. Ultrastructural data including the character-rich flagellar base area are available for *P. cinctum* and the type species of *Peridiniopsis*, *P. borgei* Lemmermann (Calado et al. 1999; Calado and Moestrup 2002). In addition, species of the marine genus *Scrippsiella* Balech ex AR Loeblich have a thecal organization that closely matches that of *P. lomnickii*; however, available ultrastructural information on *Scrippsiella* species (Bibby and Dodge 1973, 1974; Gao et al. 1989; Gao and Dodge 1991; Kalley and Bisalputra 1971; Roberts et al. 1987) is insufficient to allow the comparison of critical features and we therefore add new observations on *S. trochoidea* (F Stein) AR Loeblich.

The partial LSU rDNA sequence of *Peridinium lomnickii* was added to the database of peridinioid sequences compiled in recent contributions for the revision of *Peridinium* and allied genera (Calado et al. 2009; Craveiro et al. 2009) and used for phylogeny reconstruction with maximum likelihood and Bayesian analysis methods.

Results

Peridinium lomnickii: External Morphology

Cells of *Peridinium lomnickii* were egg-shaped, very slightly flattened dorsoventrally (Figs 1A–D, 2A,

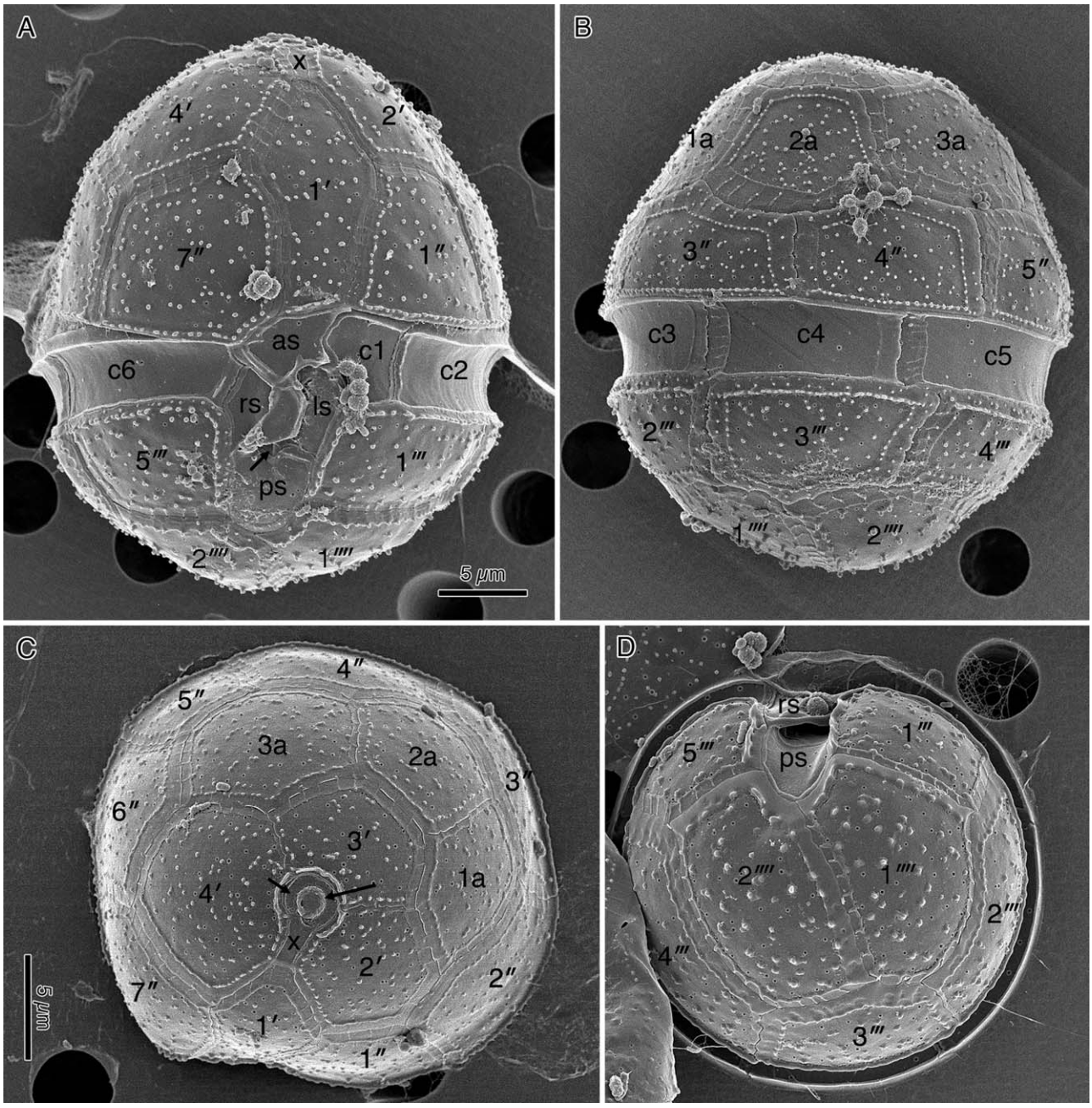

Figure 1. *Peridinium lomnickii*, SEM. Material from Sweden (A—C) and Greenland (D). The plates are marked in Kofoidian notation. **A**. Ventral view. The arrow points to the accessory plate in the sulcal region, partially covered by the right sulcal plate (rs) and x marks the canal plate near the apex. **B**. Dorsal view. Scale bar as in A. **C**. Apical view showing the apical pore complex with the canal plate (x) indenting the pore plate (small arrow) on the ventral side. The long arrow points to the rim around the cover plate. **D**. Antapical view. Scale bar as in C.

B). The cingulum was nearly equatorial, with a minor downward shift at the distal end, and divided the theca into a larger helmet-shaped epitheca and a smaller, smoothly round hypotheca (Fig. 1A, B). The sulcus did not penetrate the epitheca and ended posteriorly a little beyond the ventral edge of the antapical plates (Figs 1A, 2A, B). Cell dimensions were similar in the populations studied, from Denmark, Portugal, Sweden and Greenland, and mostly fell within the range of 27–38 μm

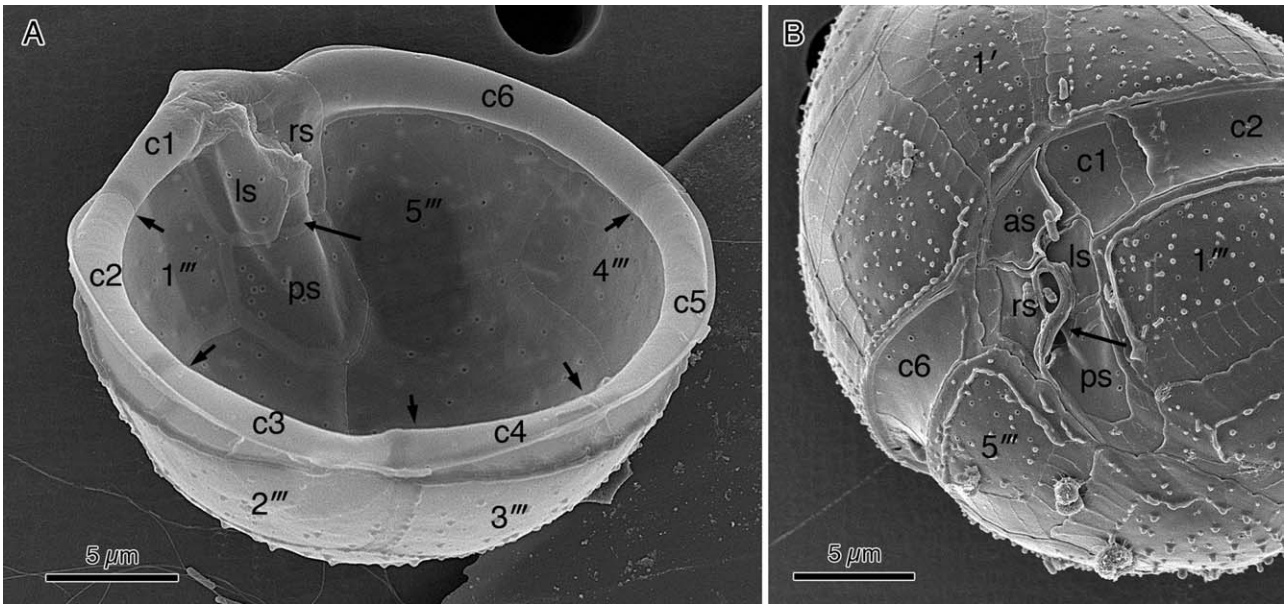

Figure 2. *Peridinium lomnickii*, SEM. Material from Greenland (A) and Sweden (B). The long arrow in both images points to the small sulcal accessory plate. **A**. Internal view of the hypotheca. Small arrows indicate the five sutures separating the six cingular plates (c1-c6). **B**. Ventral view of the sulcal region.

long and 22–32 μm wide, with a length:width ratio of 1.0–1.2.

Tabulation was the usual for this species. The arrangement of the epithecal plates was roughly symmetrical, with a slight clockwise twist of the four apical plates imposed by the larger size of plate 3a relative to the other two intercalary plates, as seen in apical view (Fig. 1C). Three platelets made up the apical pore complex; the canal plate (marked x in Fig. 1C) deeply notched the ventral side of the circular pore plate, and a distinct rim surrounded the cover plate that obstructed the pore (Fig. 1C). The cingulum contained six plates, of which the small c1 impinged on the left side of the anterior sulcal area (Figs 1A, B, 2A, B). Five plates were visible in the sulcus; four larger plates occupied anterior, posterior, left and right of the sulcal area and a small platelet was just visible between the right, left and posterior sulcal plates (Figs 1A, 2A, B). The left side of the right sulcal plate was raised in a flap-like extension covering the middle part of the sulcus (Figs 1A, D, 2B).

The surface of all major plates, both in the epitheca and in the hypotheca, was ornamented with small, conical or somewhat capitate spines that were uniformly scattered in the middle and arranged in rows along the edges of plates, especially those bordering the furrows. The spines were more prominent in the hypotheca, sometimes reaching over 0.5 μm in the antapical plates (Figs 1A–D, 2B). Plates of the apical pore complex, and cingular and sulcal plates were smooth. Circular perforations some 140 nm in diameter were randomly distributed on all thecal plates except in the apical pore complex (Figs 1A–D, 2A, B). Sutures between the plates ranged from narrow up to 4 μm wide and showed thin cross-striations with a 0.5–1 μm spacing (Figs 1B, 2B).

Ecdysed thecae broke up regularly along the anterior edge of cingulum and sulcus, sometimes remaining attached along the sulcus-epitheca boundary (Fig. 1A). An intact hypotheca with cingulum and sulcus in place is shown in Figure 2A.

General Internal Fine Structure

As seen in axial longitudinal and transverse sections of the cells, the chloroplast network was restricted to the peripheral cytoplasm whereas the central part displayed abundant dictyosomes, small vesicles and mitochondrial profiles (Fig. 3A, B). Although thylakoid-free areas were visible in some chloroplast lobes no distinct pyrenoids were found.

The ellipsoid nucleus was located at cingulum level on the dorsal-left side of the cell (Fig. 3B). Oil droplets were visible mainly in the epicone and a few starch grains in the hypocone (not shown). Vesicles with disorganized contents (so-called accumulation bodies) were present in the

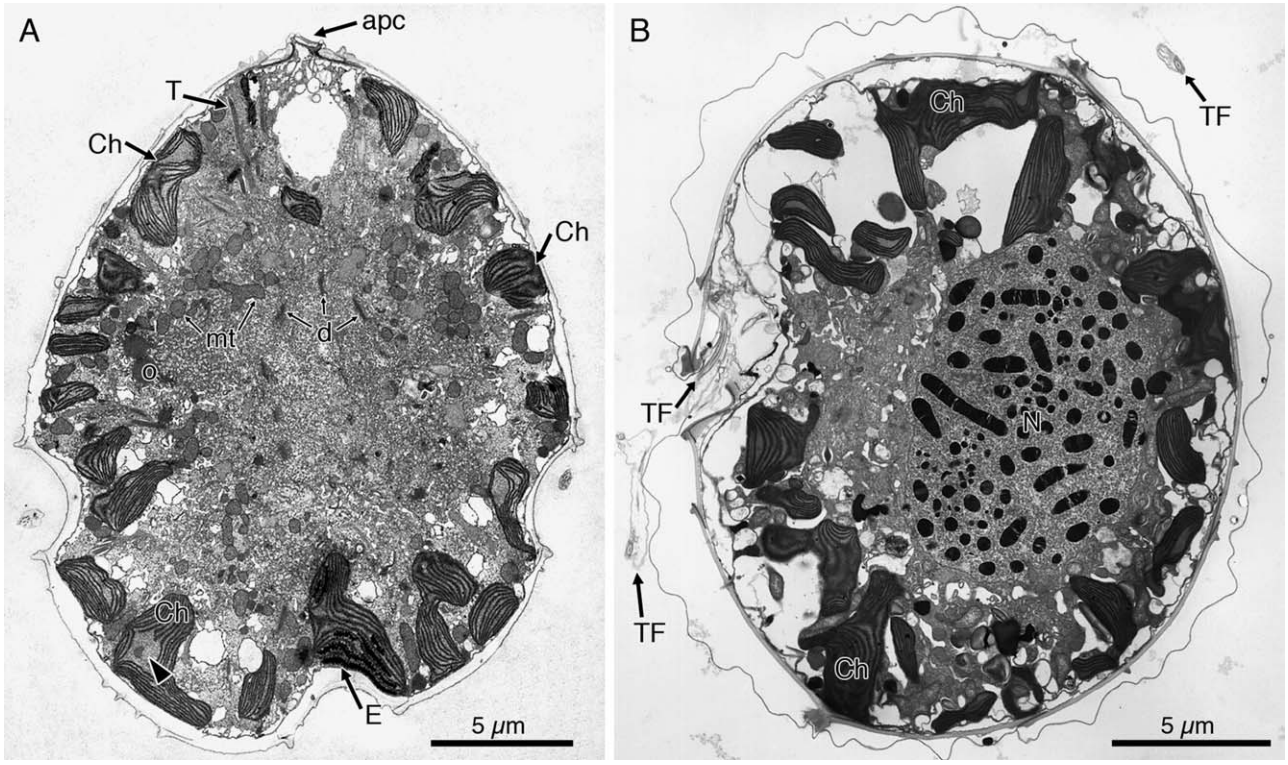

Figure 3. *Peridinium lomnickii*, TEM. General views, showing the results of two different fixation protocols. **A**. Longitudinal section, viewed from the dorsal side, showing the location near the cell surface of chloroplast lobes (Ch), some with thylakoid-free areas (arrowhead), the eyespot (E) in the sulcal region, the apical pore complex (apc), and dictyosomes (d) and mithocondria profiles (mt) in the central region. Few oil droplets (o) can be seen in the epicone. T, trichocyst. Cell fixed initially with a mixture of 1% glutaraldehyde and 0.5% osmium tetroxide **B**. Transverse section at cingulum level (apical view), near the emergence point of the transverse flagellum (TF), showing the dorsal location of the nucleus (N) and the distribution of chloroplast lobes (Ch). Initial fixation with 2% glutaraldehyde alone.

epicone of all cells examined (not shown). Trichocysts were common in the peripheral cytoplasm (Fig. 3A).

An eyespot over 5 μm long was located underneath the right-hand side of the sulcus (seen in dorsal view in Fig. 3A). It was contained in a chloroplast lobe and consisted of four or five layers of globules intercallated with thylakoid lamellae (Fig. 4A). Individual globules were 80–150 nm in diameter and the midlines of adjacent layers were 190–240 nm apart. The eyespot was overlaid with the microtubules of the longitudinal multistranded root 1, which displayed thin cross-lines in this area (Fig. 4B, C).

The ventral area, near the insertion of the flagella, showed striated fibres, microtubules and pusular elements in the form of convoluted tubes wrapped in a vesicle (Fig. 5A, B). The proximal parts of the emergent flagella were contained in a tube-like area limited externally by the flap-like extension of the right sulcal plate, which attached by means of extracytoplasmic fibres to the middle of the left sulcal plate (Fig. 5A, C).

Apical Fibrous Complex

The apical fibrous complex consisted of a group of fibres and an apparently continuous fibrous layer underlying the apical pore complex (Fig. 6A–E). Proceeding from ventral to dorsal, a group of parallel fibres extended for about 1.5 μm, increasing in number from a single fibre near the mid-ventral edge of plate x (Fig. 6A) to a seemingly continuous layer underneath the pore plate (Fig. 6B–E). A single fibre ran under the ventral-dorsal axis of the cover plate (Fig. 6C), converging with the fibrous layer under the pore plate on the ventral side and terminating near the middle of the cover plate. The dorsal side of the suture between the cover and pore plates was underlain by a curved fibre (not

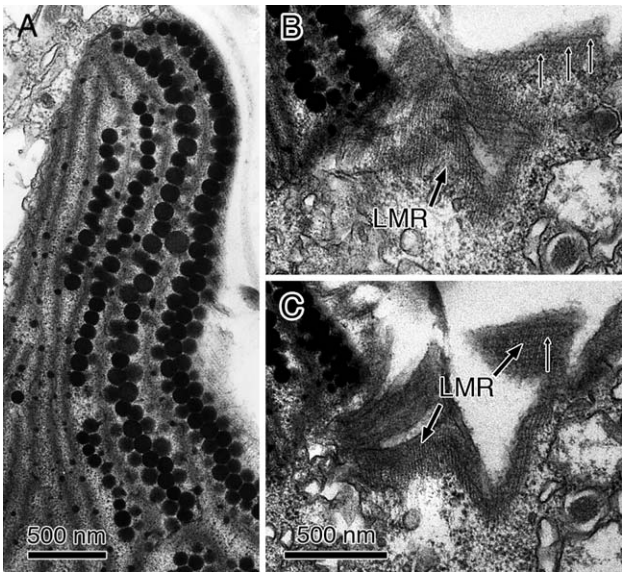

Figure 4. *Peridinium lomnickii*, TEM. Eyespot region. **A**. Eyespot-containing choroplast lobe, with four rows of globules intercalated with thylakoids. **B** and **C**. Adjacent, grazing longitudinal sections through the sulcal region showing a cross-striation (thin arrows) on the surface of the longitudinal microtubular root (LMR). Both to the same scale.

shown). Amphiesmal vesicles (or perhaps only one) were present between the cover and pore plate amphiesmal vesicles, and formed a rim around the cover plate (Fig. 6C).

In the apical region the cytoplasm was rich in 0.3–0.4 μm globose vesicles with 0.8–1 μm long tubular connections to the cover and pore plate amphiesmal vesicles (Fig. 6C). A larger vesicle was found beneath the apical region in one cell (Fig. 3A).

Peduncle and Supporting Microtubules

The relative position of basal bodies and roots, peduncle and supporting microtubules, and fibrous material making up collars and connectives is shown schematically in left view in Figure 7.

A small peduncle some 800 nm long and 350–600 nm wide protruded from the cytoplasm roughly between the two flagellar canal openings. This cytoplasmic extension was lined by a single membrane and contained one or two rows of microtubules. A complete ring of fibrous material (peduncle striated collar, PSC) surrounded the base of the peduncle and was linked to both flagellar striated collars by fibrous extensions (Figs 7, 8A–D). The small peduncle was only detected in sections of material initially fixed in a mixture containing osmium tetroxide and always appeared surrounded by sulcal plates (Figs 5A, 8A). The microtubules extended internally forming a so-called microtubular basket (MB) composed of four or five parallel rows of microtubules (Figs 7, 9A–D). Each microtubular row was composed of 8–25 microtubules (most commonly 15) and the MB had a total of 55–70 microtubules (Fig. 9E). Although vesicles were absent from the extruded peduncles examined, conspicuous elongated vesicles (EV) extended from near the peduncle base along the MB, widening from little more than a microtubule width to near 100 nm in their proximal portion (Fig. 9A–D). Vesicles and microtubules extended along the ventral surface toward the apex for about 2 μm before curving into the apical part of the cytoplasm; some 5 μm further into the cell the EV diverged slightly toward the cell's right and terminated without any obvious connection to another structure (Fig. 9). Electron-opaque material lining the inside of the wider portions of the vesicles is visible in Figure 9C. The four or five rows of the MB continued in an apical-dorsal direction for another 6 μm or so, apparently with a more windy path, and ended near the anterior side of the nucleus without visibly associating with any structure. Accumulation bodies were present near the proximal part of the MB (not shown).

Flagellar Apparatus

The arrangement of the flagellar apparatus is shown in serial sections with a dorsal-right to ventral-left orientation in Figures 10 and 11. Some flagellar roots are shown in different orientations in Figures 12 and 13.

The basal bodies formed an angle of 85–90°, with the proximal end of the transverse basal body (TB) slightly overlapping the proximal end of the longitudinal basal body (LB) (Fig. 7). Each flagellum emerged from the cytoplasm into a so-called flagellar canal, a surface depression lined by a single membrane and limited externally by a ring of fibrous material (Figs 7, 8C–D).

A row of microtubules contacted obliquely with the left base of the LB and extended underneath the sulcus toward the antapex (Figs 7, 10, 11A–D). The number of microtubules in this longitudinal microtubular root (LMR; designated r1 in Moestrup 2000) increased from about 10 near the LB (Fig. 11D) to about 35 more distally (Fig. 10C). The proximal end of the LMR was partly lined on the dorsal side by an electron-opaque layer 60 nm thick, from which thin fibres stretched out for about 120 nm toward the posterior-proximal surface of the TB (Figs 7, labelled TB-LMRc; 11D, double arrow).

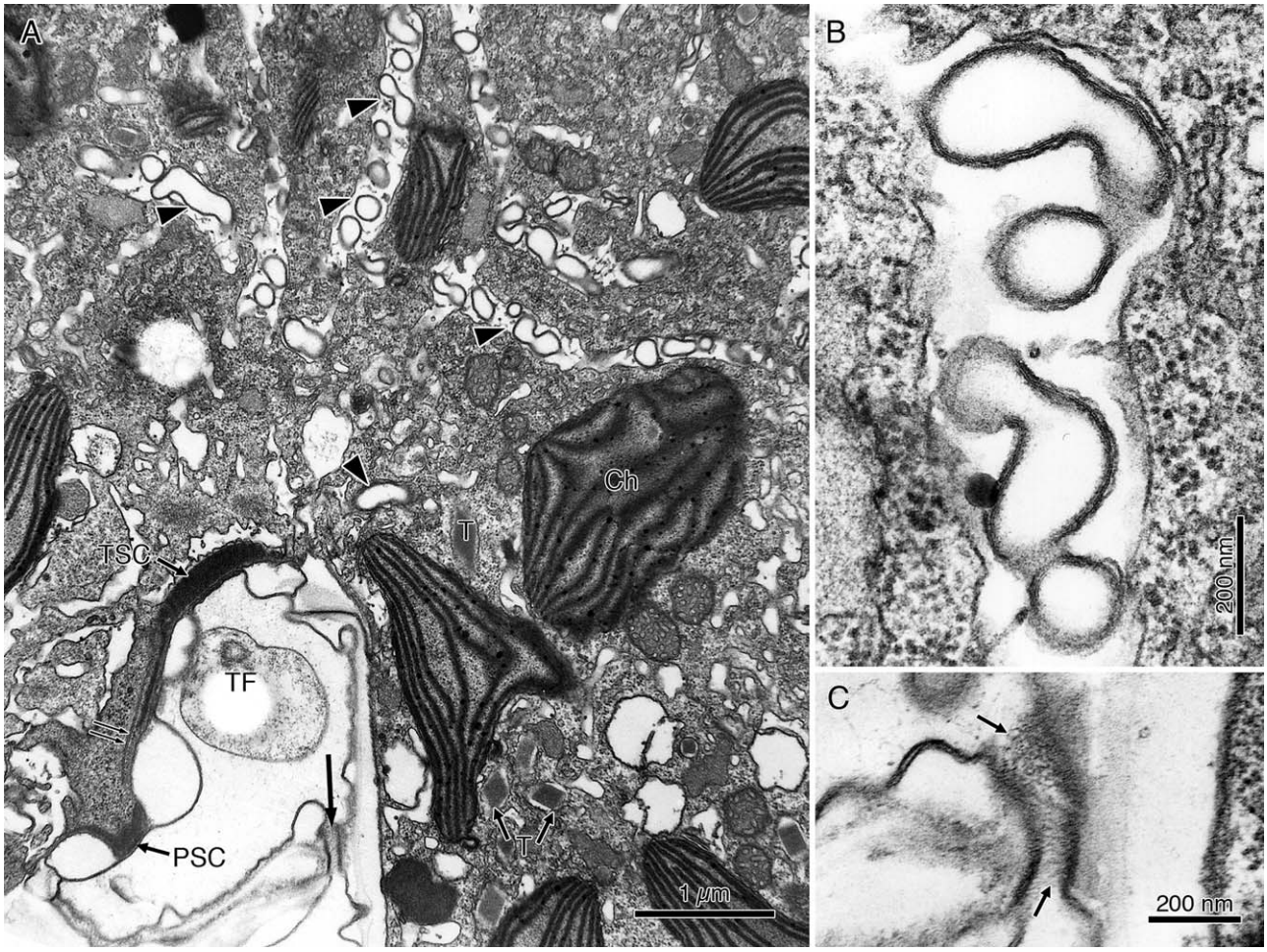

Figure 5. *Peridinium lomnickii*, TEM. **A**. Approximately ventral view showing the convoluted pusular tubes (arrowheads). One row of microtubules of the microtubular basket (double arrow) and the peduncle striated collar (PSC) are visible on the bottom-left part of the image. A tubular area surrounds the proximal part of the transverse flagellum (TF), closed externally by a connection between the plasmalemma at the edge of a sulcal plate and near the middle of another (long arrow). **B**. Higher magnification of a pusular tube and its envelopping vesicle. **C**. Detail of the thin fibres (arrows) making the connection indicated in A.

Right below this TB-LMR connective a more extensive layer of electron-opaque material covered the dorsal surface of the LMR, extended across the base of the LB and connected with the posterior face of the so-called layered connective (LC) (Figs 10C–D, 11A–C). When seen in cross-section (i.e., in longitudinal sections of the cell) the layered connective was approximately 160 nm thick, with an electron-translucent inner part some 50 nm thick limited by two distinct electron-opaque layers, each thinner than a unit membrane, and with a distinct layer of less compact electron-opaque material along the middle; two 30-nm layers of electron-opaque material formed the anterior and posterior limits of the LC, apparently linked by bands of 20-nm long fibres to the inner part of the structure (Figs 10C, D, 11A, B). The LC extended for ca. 400 nm along the left-right axis of the cell and slightly less along the ventral-dorsal axis. The anterior electron-opaque layer of the LC was continuous with similar-looking material extending around the base of the TB (Figs 10C, D, 11A–C).

A single-stranded microtubular root (SMR; r2 in Moestrup 2000) associated obliquely with the right side of the LB, extended parallel to the LMR for about 1 μm, and terminated near the connection between a pusular tube and the longitudinal flagellar canal (Figs 7, 10A–D, 11A–C).

Another root initially composed of a single microtubule extended from the anterior surface of the TB and gradually curved upward and around the ventral-right side of the transverse flagellar canal

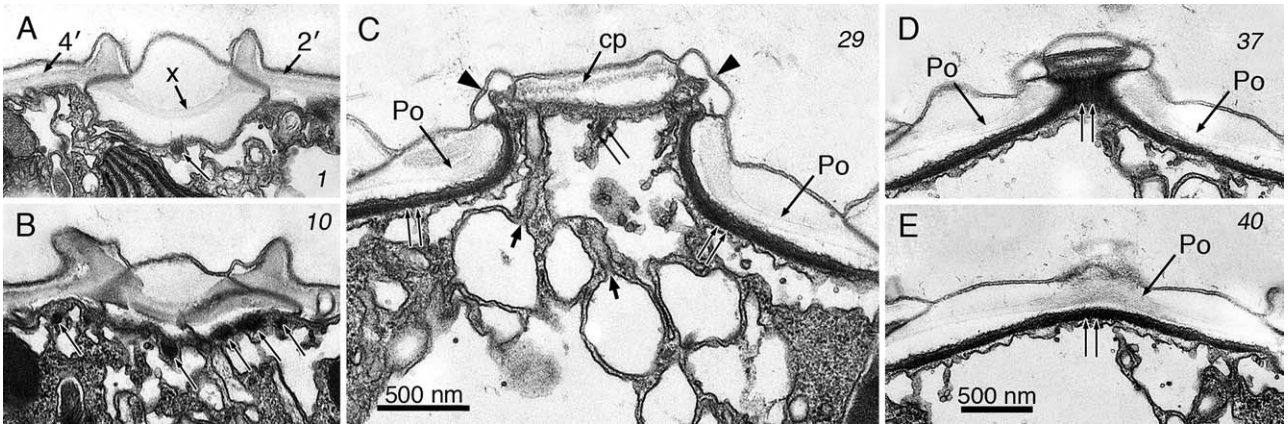

Figure 6. *Peridinium lomnickii*, TEM. Apical pore complex. Longitudinal serial sections proceeding toward the dorsal side of the cell. The small slanted numbers refer to the section number. **A**. The canal plate (x) is seen between apical plates two and four. A single fibre is visible in cross section (arrow) under the canal plate. **B**. A larger number of fibres underlying the dorsal edge of the canal plate (arrows). **C**. Section through the cover plate (cp) and the pore plate (Po). The amphiesmal vesicle forming the rim that surrounds the cp is indicated by arrowheads. Fibres underlying the pore plate and the middle of the cover plate are marked with double arrows. Several vesicles with tubular extensions converging toward the cp are marked with short arrows. **D** and **E**. Fibres on the dorsal edge of the cp and underneath the Po (double arrows). A, B, D and E to the same scale.

(TFC) for some 700 nm; this transverse microtubular root (TMR; r3 in Moestrup 2000) then slightly descended on the oposite side of the TFC, along a row of collared pits, and terminated near the emergence of a pusular tube (Figs 7, 11D–F). An extension of about 20 microtubules started at the distal part of the TMR, curved around the anterior surface of the TFC and bent toward the dorsal side, where the microtubules associated with fibrous material (Figs 7, 11D–F, 12A–D). The extension microtubules continued beyond this point for some 5 μm in the anterior direction and eventually terminated near an accumulation body and the proximal end of the MB (not shown). In the distal tract of the TMR-extension the microtubular strand closed into a flat ring and the associated fibre was no longer visible (Fig. 12E, F).

A striated fibre (transverse striated root, TSR) associated with the anterior layer of the LC and the proximal-posterior end of the TB, and extended along the dorsal side of the transverse striated collar (TSC) for up to 1.3 μm, toward the cell's left (Figs 7, 13A, B). A single microtubule (TSRM; r4 in Moestrup 2000) accompanied the TSR for most of its length (Figs 10D, 13A), but diverged from it near the proximal end (not shown).

Pusular System

The general aspect of the pusular system in the ventral area is shown in Figure 5. The pusular elements were tubular membrane-bounded compartments wrapped in a vesicle (Fig. 5B). A single tube opened at each flagellar canal (Fig. 7). The three pusular membranes were close together in the nearly straight segment that connected with each flagellar canal (Figs 10D, 11D, arrow). The tubes had an inner diameter of about 190 nm in this part. After some 1.5 μm the tubes became extensively bent and the wrapping vesicle became wider (Fig. 5A, B). The pusular tube attached to the TFC extended roughly to the ventral-left, whereas the tube linked to the LFC went to the dorsal-right side of the cell. In their terminal, inner parts the tubes seemed to flatten out and were perhaps ramified (Fig. 9D).

Cyst Morphology

Peridinium lomnickii cysts (examined mainly from culture SCCAP K-1151) were 30–35 μm long and 24–29 μm wide, with roughly the same shape as the motile cell. A strong wall, nearly 1.5 μm thick, was apparent beneath the theca of recently-formed cysts (Fig. 14A, B). Cyst contents were generally colourless except for a red body usually present in the middle of the epicone (Fig. 14B, arrow).

Scrippsiella trochoidea: Cyst Morphology

Cysts of the strain of *Scrippsiella trochoidea* examined are shown in Fig. 14C–E. They were ovoid,

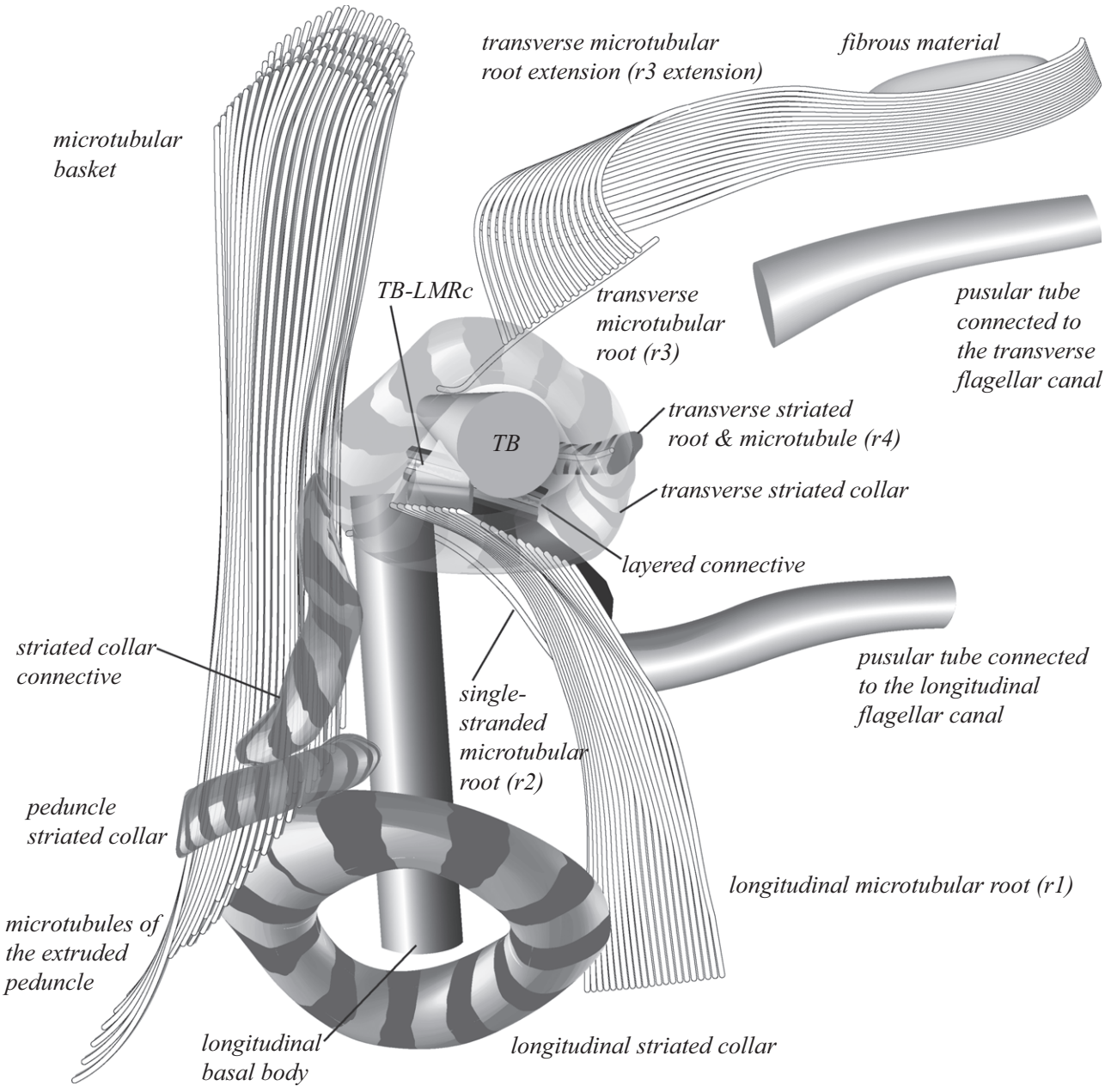

Figure 7. Schematic reconstruction of the flagellar apparatus, microtubular basket and pusular tubules of *Peridinium lomnickii*, as seen from the left side of the cell (TB, transverse basal body). The transverse and peduncle striated collars, and the fibrous connective between them are rendered transparent to show underlying structures.

39–41(–49) μm long and 27–29 μm wide, with a calcareous outer wall furnished with generally triangular spines with irregular bases and pointed or blunt tips (Fig. 14C, E). The contents were colourless except for the presence of a red body (Fig. 14D, arrow).

Fine Structure of Motile Cells

Cells were ovoid with a round hypocone and a conical epicone. General fine-structural features are shown in longitudinal and transverse sections in Figure 15A and B, respectively. Chloroplast pro-

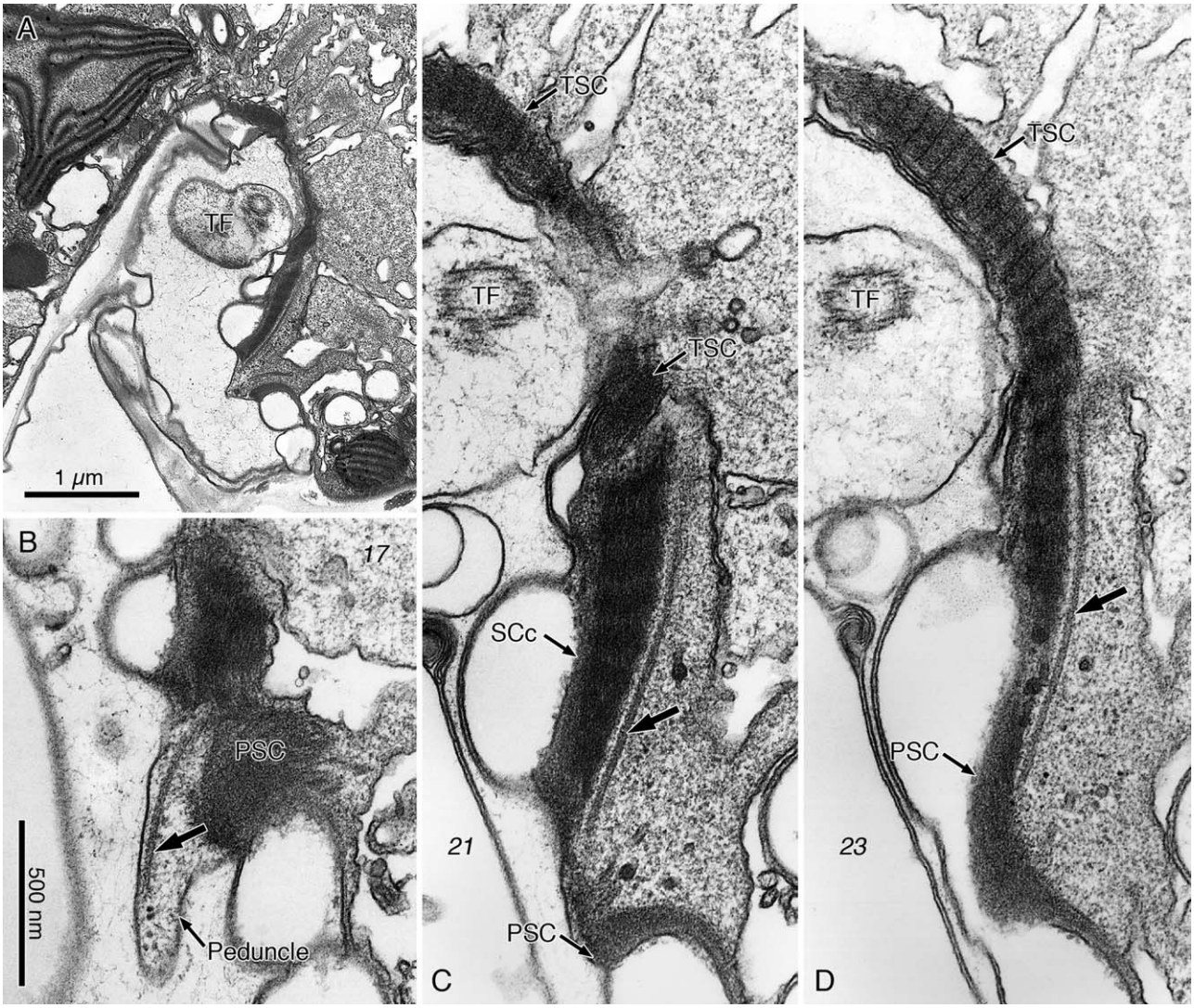

Figure 8. *Peridinium lomnickii*, TEM. Peduncle area. **A**. Emergence area of the peduncle seen from dorsal-left. TF, transverse flagellum. **B–D**. Non-adjacent, longitudinal serial sections from a different cell viewed with a similar perspective. Small slanted numbers indicate the section number. A small peduncle formed by cytoplasm and microtubules (arrow) and limited by a single membrane extends through the peduncle striated collar (PSC). A striated collar conective (SCc) links the transverse striated collar (TSC) and the PSC. The supporting microtubules continue within the cytoplasm parallel to the collars and connective (arrow).

files, few in number but relatively large, lined most of the cell surface; thylakoid-free chloroplast areas were visible here and there and at least two larger, starch-covered pyrenoids projected inward from the peripheral lobes (Fig. 15A, B). The pyrenoids were penetrated by tubular, membrane-bounded structures, single or paired, that seemed to be continuous with thylakoids (Fig. 15F, G). An eyespot up to 1.5 μm long, composed of 1–2 rows of globules, was present in a chloroplast lobe in the sulcal region (Fig. 15E). Longitudinal sections through the cell apex showed thin fibres flanking the slightly projecting apical pore region (Fig. 15C, f). The nucleus was located at the central-dorsal part of the cell, at cingulum level (Fig. 15B). A large part of the right mid-ventral cytoplasm was occupied by the pusule, composed of tubular and flattened, ramified vesicles that radiate from the flagellar base area (Fig. 15B, D).

Although four cells were examined, neither a microtubular basket nor a microtubular strand that could be associated with a peduncle were found.

Figure 9. *Peridinium lomnickii*, TEM. Microtubular basket (peduncle-related microtubules). Same series of sections as Fig. 8B–D (except the insert E). Small slanted numbers refer to the section number. **A–C**. Four rows of microtubules (arrows) parallel to a group of elongated vesicles (EV). All to the same scale. **D**. The microtubules (arrow) and the elongated vesicles (EV) diverge as they continue toward the inner cytoplasm of the epicone. **E**. Transverse section through the inner portion of the microtubular basket of another cell, some 12 μm away from the area of emergence of the peduncle, showing five nearly parallel rows of microtubules.

The flagellar apparatus contained the typical peridinioid elements, including a LC (Fig. 16A), and is not described further. However, the areas of emergence of both flagella were distinctive in having what appeared to be 5–6 platelets defining narrow, cylindrical canals that the flagella seemed to squeeze through; these platelets were contained in vesicles with the same appearance as the amphiesmal vesicles of other plates, but they were positioned in layers and were made of a distinct, somewhat fibrous-looking material (Fig. 16).

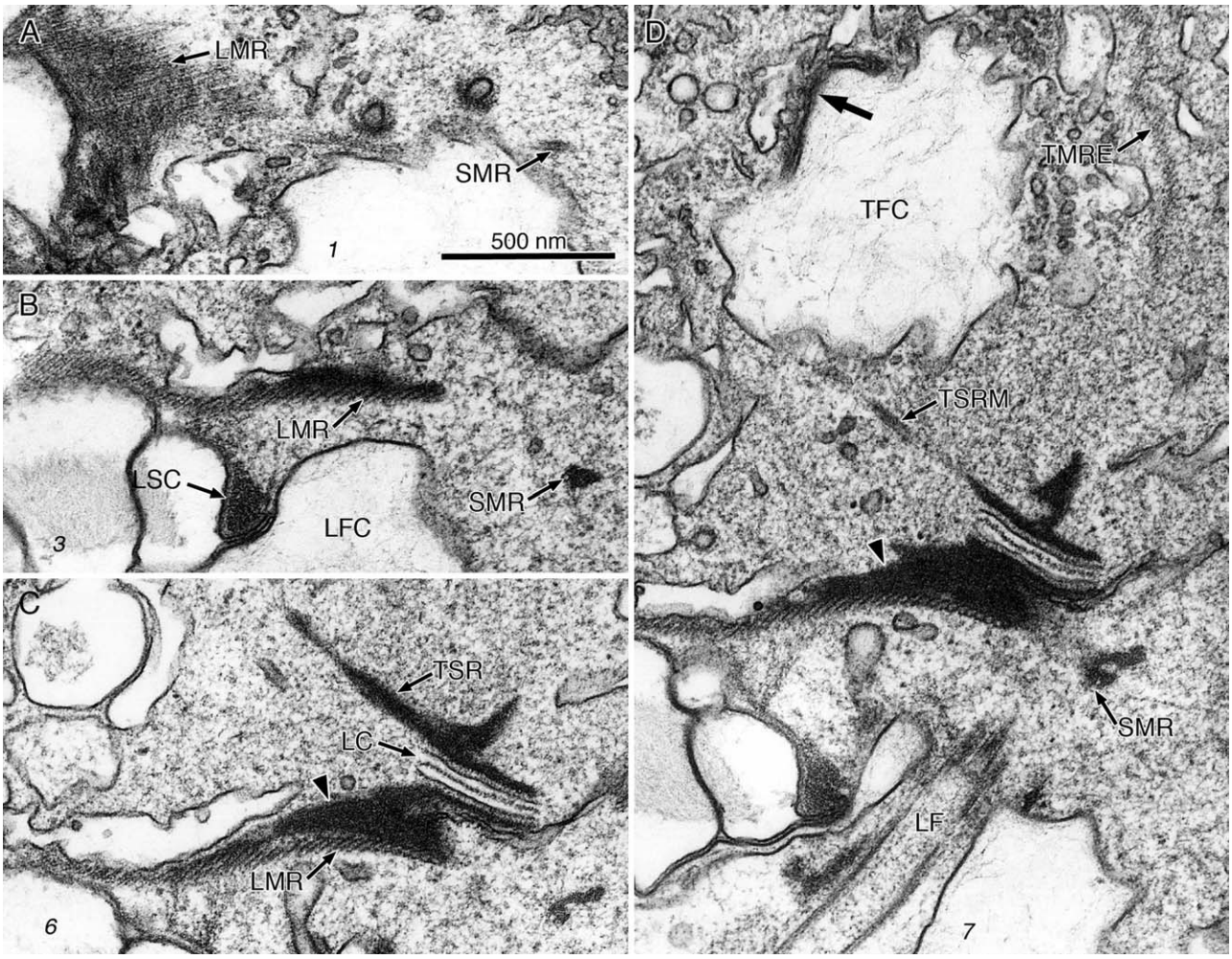

Figure 10. *Peridinium lomnickii*, TEM. Flagellar apparatus. **A–D**. Non-adjacent, nearly longitudinal serial sections proceeding toward the ventral side of the cell, in dorsal view. Small slanted numbers refer to the section number. All to the same scale. The single-stranded microtubular root (SMR) follows a path roughly parallel to the longitudinal microtubular root (LMR) and is visible in all sections. Electron-opaque material covering the dorsal side of the LMR is indicated in C and D (arrowhead). A pusular tube (marked with an arrow in D) connects with the transverse flagellar canal (TFC). LC, layered connective; LF, longitudinal flagellum; LFC, longitudinal flagellar canal; LSC, longitudinal striated collar; TMRE, the transverse microtubular root extension; TSR, transverse striated root; TSRM, microtubule of the transverse striated root.

Molecular Phylogeny

On the basis of the morphological, ultrastructural and molecular results *Peridinium lomnickii* is transferred below to a new genus. Its LSU rDNA sequence was therefore registered in GenBank under the species name *Chimonodinium lomnickii* and this name is used hereafter. In the LSU rDNA based phylogeny including 32 dinoflagellate genera *Peridinium aciculiferum* and *Chimonodinium lomnickii* form two early diverging lineages related to *Thoracosphaera*, *Tyrannodinium* and the other three pfiesteriaceans (Fig. 17). This cluster of dinoflagellates is well supported in terms of posterior probabilites (PP = 1.0) but has only little support from bootstrap analysis (BS = 60%). The sister group relationship between these 7 genera of dinoflagellates and the group containing *Scrippsiella* spp. and *Peridiniopsis polonica* is well supported both in terms of posterior probabilities and bootstrap values (PP = 0.98 and BS = 97%). However, the phylogenetic positioning of *Chimonodinium* as a sister group to *Thoracosphaera, Tyrannodinium* and

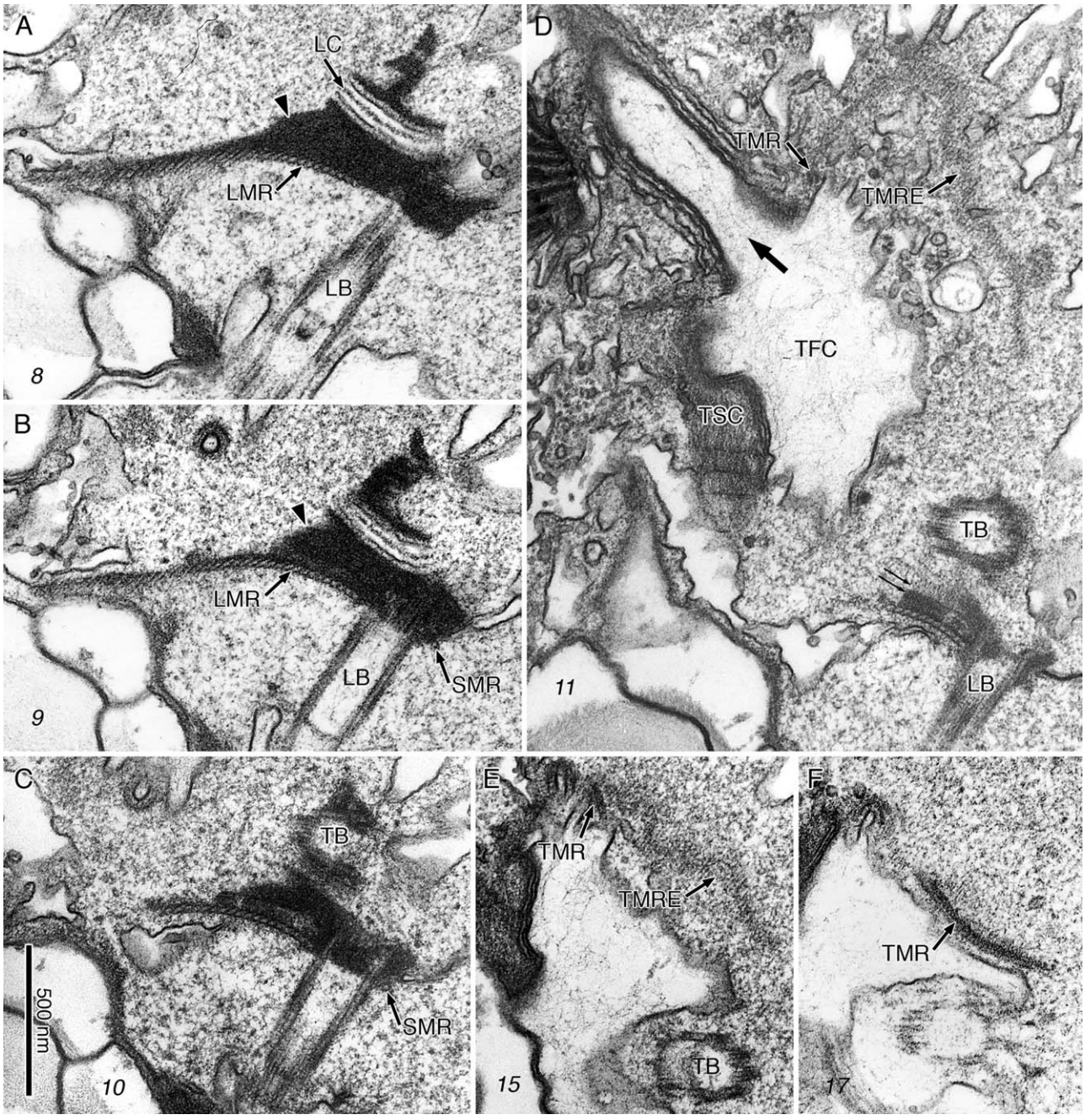

Figure 11. *Peridinium lomnickii*, TEM. Flagellar apparatus. **A–F**. Continuation of the series of sections shown in Fig. 10. Small slanted numbers refer to the section number. All to the same scale. The single-stranded microtubular root (SMR) ends in the right-proximal side of the longitudinal basal body (LB), in an almost perpendicular orientation in relation to it (C). The electron-opaque material (arrowheads in A and B) on the dorsal side of the longitudinal microtubular root (LMR) connects with the layered connective (LC). A pusular tube (arrow) connecting with the transverse flagellar canal (TFC) and a connective between the LMR and the transverse basal body (TB) (double arrow) are seen in D. The transverse microtubular root (TMR) and the microtubules which it nucleates (TMRE) are visible in D–F.

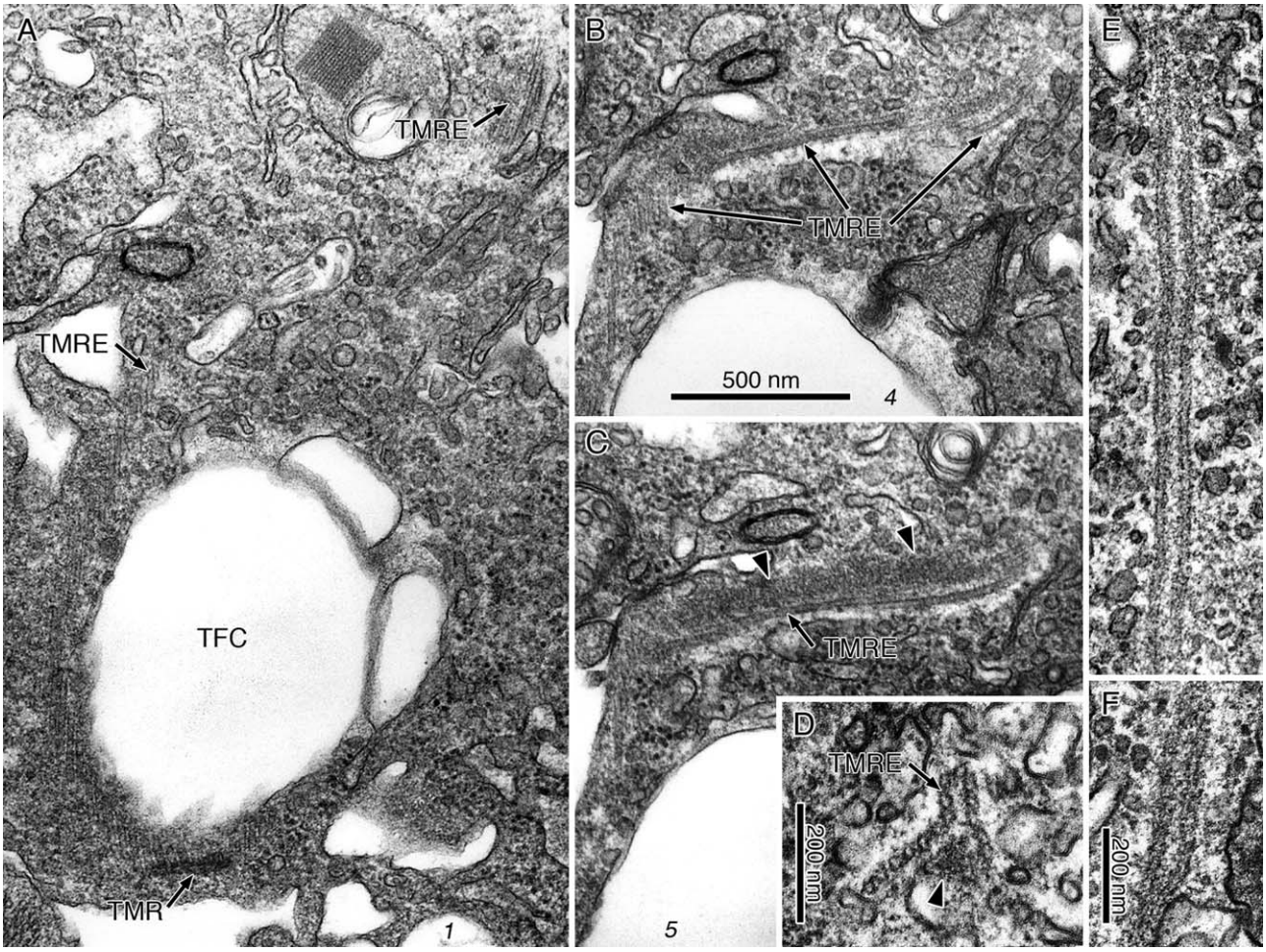

Figure 12. *Peridinium lomnickii*, TEM. Flagellar apparatus, transverse microtubular root extension (TMRE). **A–C**. Non-adjacent, transverse serial sections, in apical view, of the transverse microtubular root (TMR) and TMRE. The TMR is seen in A, ventral to the transverse flagellar canal (TFC). The TMRE extends along the right side of the TFC toward the back of the cell and then curves to the cell's left. In the dorsal side of the LFC the dorsal face of the TMRE associates with fibrous material (arrowheads). Small slanted numbers refer to the section number. All to the same scale. **D–F**. Three different aspects of the TMRE in longitudinal sections of the same cell. In D the TMRE is seen in cross section with the microtubules forming an open ring wrapped around fibrous material (arrowhead), some 3 μm from the basal body area. An approximately longitudinal section of the TMRE is shown in E. In the oblique view shown in F the TMRE seems to form a closed ring. E and F are about 5 μm away from the basal body area. A–C and E to the same scale.

other pfiesteriaceans is not supported (PP = 0.59 and BS<50%).

To infer the phylogeny of *Chimonodinium lomnickii* in greater detail a second data matrix containing 13 of the most closely related dinoflagellates to *C. lomnickii* was analyzed using Bayesian and maximum likelihood analyses. The analyses corresponded to those performed on the first alignment (see Methods). However, due to the close relationship between these dinoflagellates we could include the otherwise highly divergent domain D2 sensu Lenears et al. (1989) and the second alignment thus comprised 1291 base pairs including introduced gaps. The topology obtained from Bayesian analysis is illustrated as an unrooted tree in Figure 18. It revealed a posterior probability of 0.9 for *Chimonodinium lomnickii* forming a sister taxon to *Thorachosphaera* and the four genera of pfiesteriaceans included in this analysis. The lack of support from maximum likelihood (ML) for this branching pattern is due to the fact that *C. lomnickii* and *Peridinium aciculiferum* formed a sister

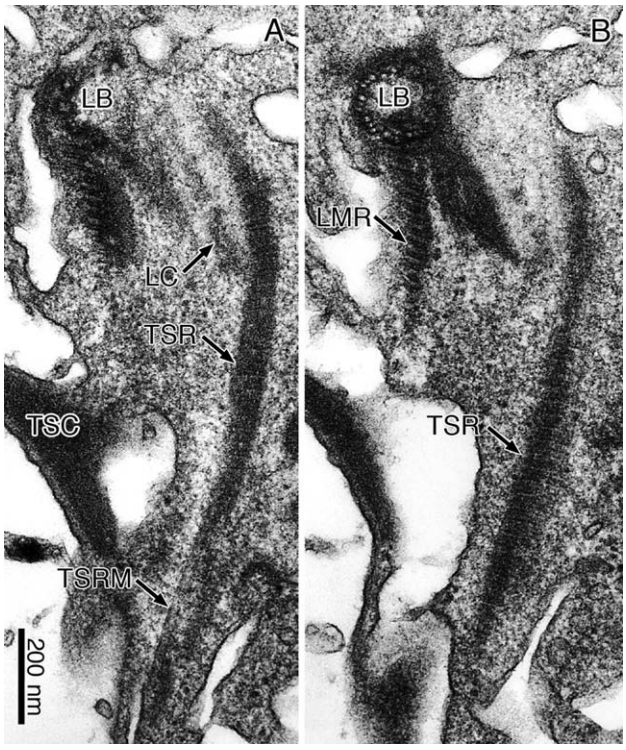

Figure 13. *Peridinium lomnickii*, TEM. Flagellar apparatus, transverse striated root (TSR). **A** and **B**. Apical view of adjacent transverse sections, somewhat tilted to show the longitudinal basal body (LB) in cross section. The transverse striated root microtubule (TSRM) is visible along the TSR. LC, layered connective; LMR, longitudinal microtubular root; TSC, transverse striated collar. Both figures to the same scale.

group to *Thorachosphaera* and the pfiesteriaceans when using ML (tree not shown). This relationship was also proposed by the ML analysis of the first alignment that included a diverse assemblage of dinoflagellates (tree not shown). The overall tree topology for the second alignment was otherwise similar to that retrieved from phylogenetic analyses of the first alignment; compare Figures 17 and 18. Despite proposing a slightly different phylogeny for *Chimonodinium* both analyses (Bayesian and ML) indicate that it is distantly related to *Peridinium cinctum*, the type species of the genus.

Sequence Divergence

Sequence divergences were estimated by pairwise comparison based on 1266 base pairs of the LSU rRNA gene in *Chimonodinium lomnickii* and a representative assemblage of nine of the most closely related dinoflagellates, both as

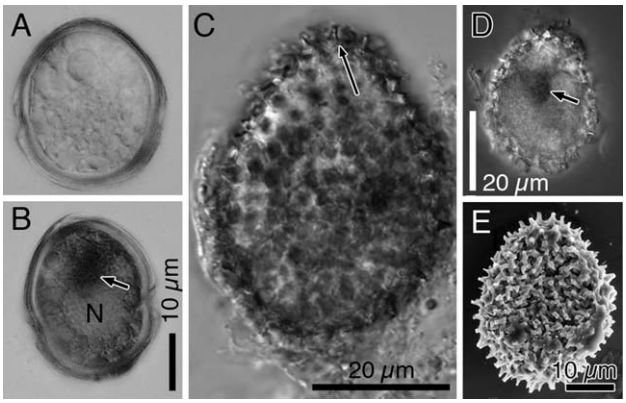

Figure 14. Cysts of *Peridinium lomnickii* from Sweden (A–B) and of *Scrippsiella trochoidea* (C–E) from culture KF2N16. **A** and **B**. Light micrographs of two cysts with thick, unornamented wall. The cyst in B shows a dark red body (arrow) and the nucleus (N). Both images to the same scale. **C** and **D**. Light micrographs of calcareous cysts with triangular spines (long arrow in C) and a red body (short arrow in D). **E**. SEM of an ovoid calcareous cyst.

uncorrected distances (P-values from PAUP*) and calculated using the Kimura-2-parameter model (slightly higher percentage values). The overall sequence divergence in the LSU rRNA genes of *C. lomnickii* and *P. aciculiferum* is < 2%, whereas the sequence divergence between *C. lomnickii/P. aciculiferum* and *Scrippsiella trochoidea* is 3.5–3.7%. There is a ≈ 5-6% sequence divergence between *C. lomnickii* and *Tyrannodinium*, *Thoracosphaera*, *Pfiesteria* and *Peridiniopsis polonica*. Sequence divergence between *C. lomnickii* and the type species of *Peridinium* (*P. cinctum*) is 14 or 15.7%, depending on the method used to estimate the divergence. Both sequence divergence estimates between *C. lomnickii* and *P. borgei* are slightly smaller, but still relatively large: 9.8% and 10.7%.

Taxonomic Descriptions

Chimonodinium Craveiro, Calado, Daugbjerg, Gert Hansen et Moestrup gen. nov.

Dinoflagellata autotrophica, thecata, non parasitica. Formula kofoidiana thecarum Po, cp, x, 4′, 3a, 7″, 6c, 5s, 5‴, 2⁗. Lobi chloroplasti in strato externo cytoplasmatis distributa, sine pyrenoidibus. Stigma in lobo chloroplasti subter sulcum sito. Fila microtubularia peduncularia quadrifariam vel quinquefariam (alveus microtubularis dictus), ad extremum ventrales vesiculis fuscis (per microscopium electronicum visae) concomitatis. Pusula tubularis saltem prope canales flagellares, ad pars profunda convoluta et complanata. Theca cinguli anteriorem marginem dehiscens. Cysta ovoidea vel ellipsoidea cum pariete crassa non calcarea.

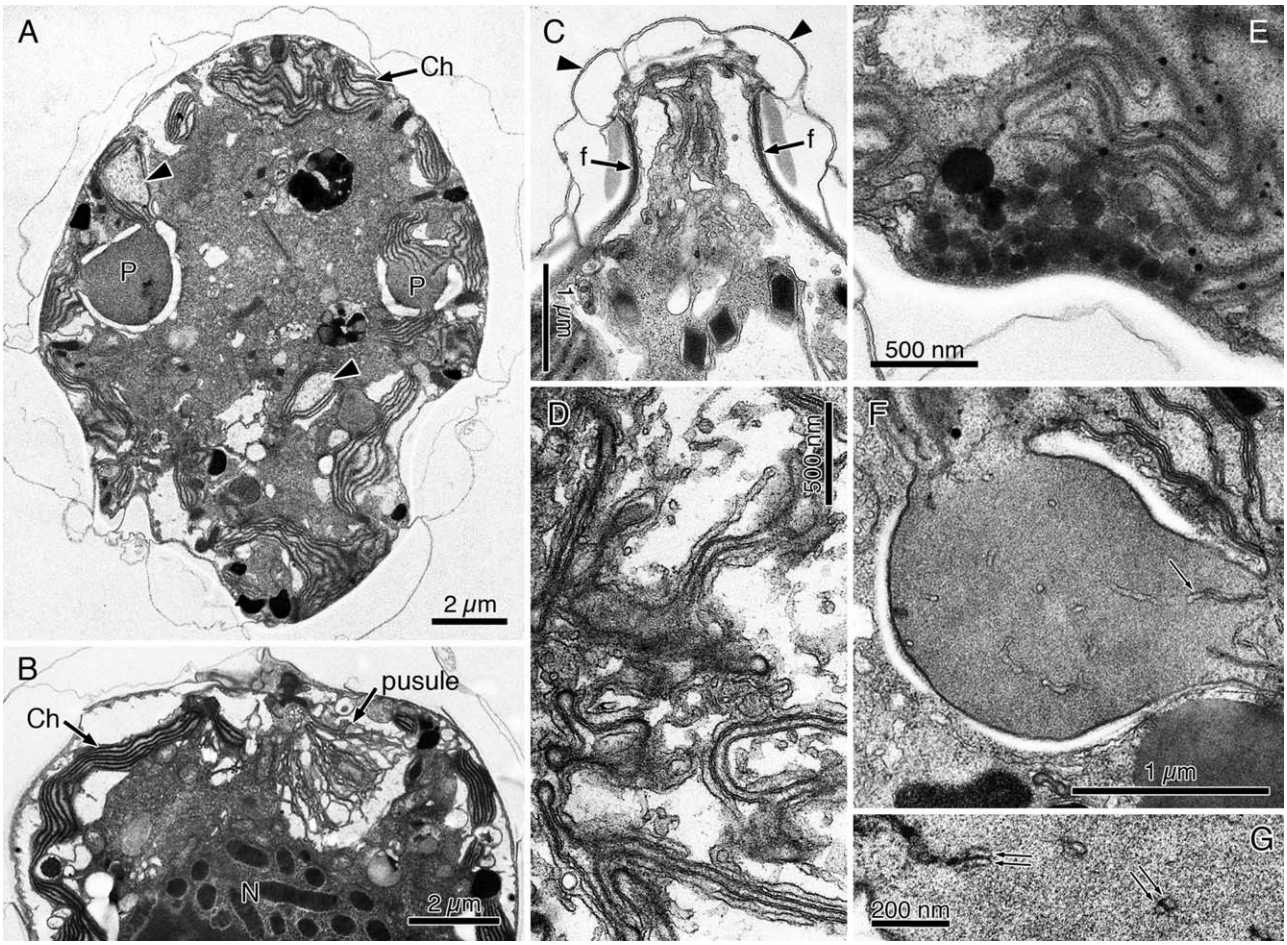

Figure 15. *Scrippsiella trochoidea*, TEM. **A.** Longitudinal section showing the general organization. Note the multiple-stalked pyrenoids (P) with sheaths of starch. Ch, chloroplast lobes. Areas of chloroplast lobes without thylakoids are indicated by arrowheads. **B**. Transverse section at cingulum level (apical view), showing the pusule and the nucleus (N). **C**. Longitudinal section through the somewhat projecting apical pore complex, showing fibres (f) of the apical fibrous complex and amphiesmal vesicle profiles (arrowheads) between the vesicles containing the pore plate and the cover plate. **D**. Detail of the pusule with the appearance of flat vesicles. **E**. Eyespot formed by a row of globules located in a chloroplast lobe. **F**. Multiple-stalked pyrenoid with tubular structures apparently continuous with the thylakoids (arrow). **G**. Detail of the pyrenoid matrix with simple or double (double arrow) tubular structures.

Typus generis: *Chimonodinium lomnickii* (Wołoszyńska) Craveiro, Calado, Daugbjerg, Gert Hansen et Moestrup comb. nov., hic designatus.

Thecate, autotrophic free-living dinoflagellates. Kofoidian plate formula: Po, cp, x, 4′, 3a, 7′′, 6c, 5 s, 5′′′, 2′′′′. Chloroplast lobes near the surface, not connected in the cell centre, without distinct pyrenoids. Eyespot located in a chloroplast lobe beneath the sulcus. Small extruded peduncle present, supported by a microtubular basket of 4 or 5 rows of microtubules extending into the anterior part of the epicone, accompanied in their distal part by elongated vesicles with electron-opaque contents. Pusular system formed by two vesicle-wrapped tubes, each one connected to one of the flagellar canals; tubes convoluted and flat in the more internal cytoplasm. Dividing or ecdysing cells exiting the theca through an opening along the anterior edge of the cingulum. Resting cyst oval to ellipsoid, with a non-calcareous, thick wall.

Type species: *Chimonodinium lomnickii* (Wołoszyńska) Craveiro, Calado, Daugbjerg, Gert Hansen et Moestrup comb. nov., designated here.

Etymology: from Greek χειμων, "winter", after Wołoszyńska's original notes on the period of greatest abundance of the type species. The termination *–dinium*, originally from Greek δινη, "vortex", is common in names of dinoflagellates.

Chimonodinium lomnickii (Wołoszyńska) Craveiro, Calado, Daugbjerg, Gert Hansen et Moestrup comb. nov.

Figure 16. *Scrippsiella trochoidea*, TEM. Exit pores of the flagella. **A**. Longitudinal flagellum (LF) exiting through a canal lined by at least four platelets (pl) in a more internal position relative to the surrounding sulcal plates. The appearance of the platelets is consistently different from that of the outer thecal plates (arrowheads). LC, layered connective; LMR, longitudinal microtubular root; LSC, longitudinal striated collar. **B**. Transverse flagellum (TF) squeezed in a canal formed by platelets (pl). TSC, transverse striated collar.

Basionym: *Peridinium lomnickii* Wołoszyńska 1916, Bull Int Acad Sci Cracovie, Cl Sci Math Nat, sér. B 1915 (8–10), p. 267, pl. 10, figs 25–29.

Homotypic synonym: *Glenodinium lomnickii* (Wołoszyńska) Er. Lindemann (1925, pp 162, 168, 169).

Heterotypic synonym: *Peridinium lomnickii* var. *punctulatum* Er. Lindemann (1924, p. 436, pl. 21, figs 1–6; '*punktulatum*').

A representative strain of this species was deposited at the Scandinavian Culture Collection of Algae and Protozoa with the strain number SCCAP K-1151.

Chimonodinium lomnickii var. ***splendidum*** (Wołoszyńska) Craveiro, Calado, Daugbjerg, Gert Hansen et Moestrup comb. nov.

Basionym: *Peridinium lomnickii* var. *splendidum* Wołoszyńska 1916, Bull Int Acad Sci Cracovie, Cl Sci Math Nat, sér. B 1915 (8–10), p. 268, pl. 10, figs 30–40 ('*splendida*').

Homotypic synonym: *Glenodinium lomnickii* var. *splendidum* (Wołoszyńska) Er. Lindemann (1928, p. 260).

Chimonodinium lomnickii var. ***wierzejskii*** (Wołoszyńska) Craveiro, Calado, Daugbjerg, Gert Hansen et Moestrup comb. nov.

Basionym: *Peridinium wierzejskii* Wołoszyńska 1916, Bull Int Acad Sci Cracovie, Cl Sci Math Nat, sér. B 1915 (8–10), p. 269, pl. 11, figs 1–8.

Homotypic synonym: *Glenodinium lomnickii* var. *wierzejskii* (Wołoszyńska) Er. Lindemann (1928, p. 260).

Discussion

A Brief Note on the Taxonomy of *Chimonodinium*

The populations we report on closely match the original description of *Peridinium lomnickii* (Wołoszyńska 1916), including the distinct size difference between epi- and hypotheca. *Peridinium wierzejskii* was described in the same article with features very similar to *P. lomnickii*, but more spherical (i.e., less elongate and less flattened dorsoventrally) and with epi- and hypotheca of the same size (Wołoszyńska 1916). The exiguity of the features separating the two taxa was noted by Lindemann (1920, 1924, 1925). However, after transferring *P. lomnickii* to *Glenodinium* because of the indistinctness of thecal plates in intact specimens, Lindemann (1928) recognized *P. wierzejskii* at variety level. Lefèvre (1932) retained this group of taxa in *Peridinium* and recognized *P. wierzejskii* as an independent species on the basis of the morphological differences originally given by Wołoszyńska (1916), and was followed by subsequent monographers (e.g., Huber-Pestalozzi 1950; Schiller 1935; Starmach 1974). Popovský and Pfiester (1990) recognized it again as a variety under the name "P. lomnickii var. wierzejskii (Wołoszyńska) Lindemann", a combination not validly published.

Peridinium lomnickii var. *splendidum* was originally described as a larger, much more flattened form than typical *P. lomnickii*, with thick borders to the furrows and an asymmetry derived from a right cell side larger than the left (Wołoszyńska 1916). The variety has been generally recognized (e.g., Huber-Pestalozzi 1950; Lefèvre 1932; Schiller 1935; Starmach 1974), but not reported. Although it is tempting to consider all these taxa as variations within the life cycle of a single species, as done by Grigorszky et al. (2003a), to reliably merge them as synonyms it would be important to recognize cells fitting the diagnostic characters given for *P. wierzejskii* and *P. lomnickii* var. *splendidum* within populations of *P. lomnickii* (preferably in clonal culture), and not only a gradation in thecal thickness. However, even in thecae containing cysts, which presumably developed form the planozygote

stage, we did not find the large size, the dorsoventral flattening or the asymmetry described for var. *splendidum*; nor could we demonstrate spherical cells with equal-sized epi- and hypotheca in the populations we studied.

The citation of *Chalubinskia tatrica* Wołoszyńska as a synonym of *P. lomnickii*, as done by Popovský and Pfiester (1990) and Grigorszky et al. (2003a), is unjustified. Both the species and the genus *Chalubinskia* Wołoszyńska were based on a single empty theca, which the author decided to describe because of the uniqueness of having a hypotheca with three post-cingular and a single antapical plate (Wołoszyńska 1916, p. 276, pl. 13, figs 1–8). The specimen was probably abnormal and the genus ill founded (Bourrelly 1970; Schiller 1935). Although the identity of *C. tatrica* with *P. lomnickii* was mentioned as possible (Schiller 1935), the relatively elongate outline, the somewhat produced apex, the smooth theca and the presence of stout spines on the edges of hypothecal plates are much more suggestive of *P. aciculiferum* Lemmermann, as noted by Wołoszyńska (1936, p. 195).

General Structure of *C. lomnickii*

The general features of *C. lomnickii* were typical for dinoflagellates. The eyespot was of type A (Moestrup and Daugbjerg 2007), with an unusually large number of layers of globules, surpassed only by *Peridiniopsis borgei*, which, however, differs in being overlaid by a vesicle with a layer of brick- or crystal-like units (Calado and Moestrup 2002). The significance of the thin cross-lines on the ventral surface of the LMR in the sulcal area is unknown; similar lines were reported from the woloszynskioids *Prosoaulax lacustris* (F. Stein) Calado et Moestrup, *Jadwigia applanata* Moestrup, K. Lindberg et Daugbjerg, and *Tovellia coronata* (Wołoszyńska) Moestrup, K. Lindberg et Daugbjerg, but also from the peridinioid *Tyrannodinium berolinense* (Lemmermann) Calado, Craveiro, Daugbjerg et Moestrup (Calado et al. 1998; Lindberg et al. 2005; Roberts et al. 1995a; Wedemayer and Wilcox 1984).

The flagellar apparatus showed all the regular features of peridinioids, notably the single microtubule that associates with the right-hand side of the LB (SMR, r2), of general occurrence in peridinioids and gonyaulacoids, and the layered connective, only found in peridinioids, that presumably takes up the function of the striated connective between LMR and TSR found in other dinoflagellate groups (Calado et al. 2006, 2009). The band of thin fibres extending from electron-opaque material on the dorsal side of the LMR toward the TB (TB-LMRc) is in the position of the well-defined fibres that link the same flagellar apparatus components in *P. borgei*, *Tyrannodinium berolinense* and *Palatinus apiculatus* (Ehrenberg) Craveiro, Calado, Daugbjerg et Moestrup (Calado and Moestrup 2002; Calado et al. 2009; Craveiro et al. 2009).

In a review of apical pore complexes of Peridiniaceae based on SEM, Toriumi and Dodge (1993) included the rim around the pore (between the pore plate and the actual pore, or the cover plate if it has not detached) as a constant feature in the group. Judging from its location and size, the profiles of amphiesmal vesicles shown on the edges of the cover plate in *C. lomnickii* (Fig. 6C) correspond to the rim visible in SEM. The presence in the apical pore complex of amphiesmal vesicles additional to the ones containing the plates has not been reported previously, although amphiesmal profiles matching the ones shown here are visible in Roberts et al. (1987) in their figure 3, representing *Heterocapsa pygmaea* A.R. Loeblich, R.J. Schmidt et Sherley, and especially in their figure 14, representing *Scrippsiella sweeneyae* A.R. Loeblich. The same aspect is present in our material of *S. trochoidea* (Fig. 15C). Although further examination of apical pores of dinoflagellates by TEM is necessary to evaluate the occurrence of supplementary amphiesmal vesicles, examination of published material suggests that they are absent in some gonyaulacoids (e.g., Hansen et al. 1996). The inclusion of *C. lomnickii* in a group of species with the pore plate not indented by the canal plate (Toriumi and Dodge 1993), contrary to the observations we report here, is not documented by the figure given, which does not show the boundary between the relevant plates (Toriumi and Dodge 1993, fig. 27), and we regard it as a mistake.

Comparison with *Peridinium*, *Palatinus* and *Peridiniopsis*

External cell features pertaining to *Peridinium* sensu stricto are those shared by the type species, *P. cinctum*, with other species in groups cinctum and willei, which differ essentially in degree of symmetry of the epithecal tabulation (Craveiro et al. 2009). Internal fine structure, including the flagellar base area, is known only from *P. cinctum* in enough detail for comparison with *Chimonodinium* (Calado et al. 1999). Both internal and external detailed analyses are available from the type species of *Palatinus* Craveiro, Calado, Daugbjerg et Moestrup, *P. apiculatus*, and *Peridiniopsis*, *P. borgei* (Calado and Moestrup 2002; Craveiro et al. 2009).

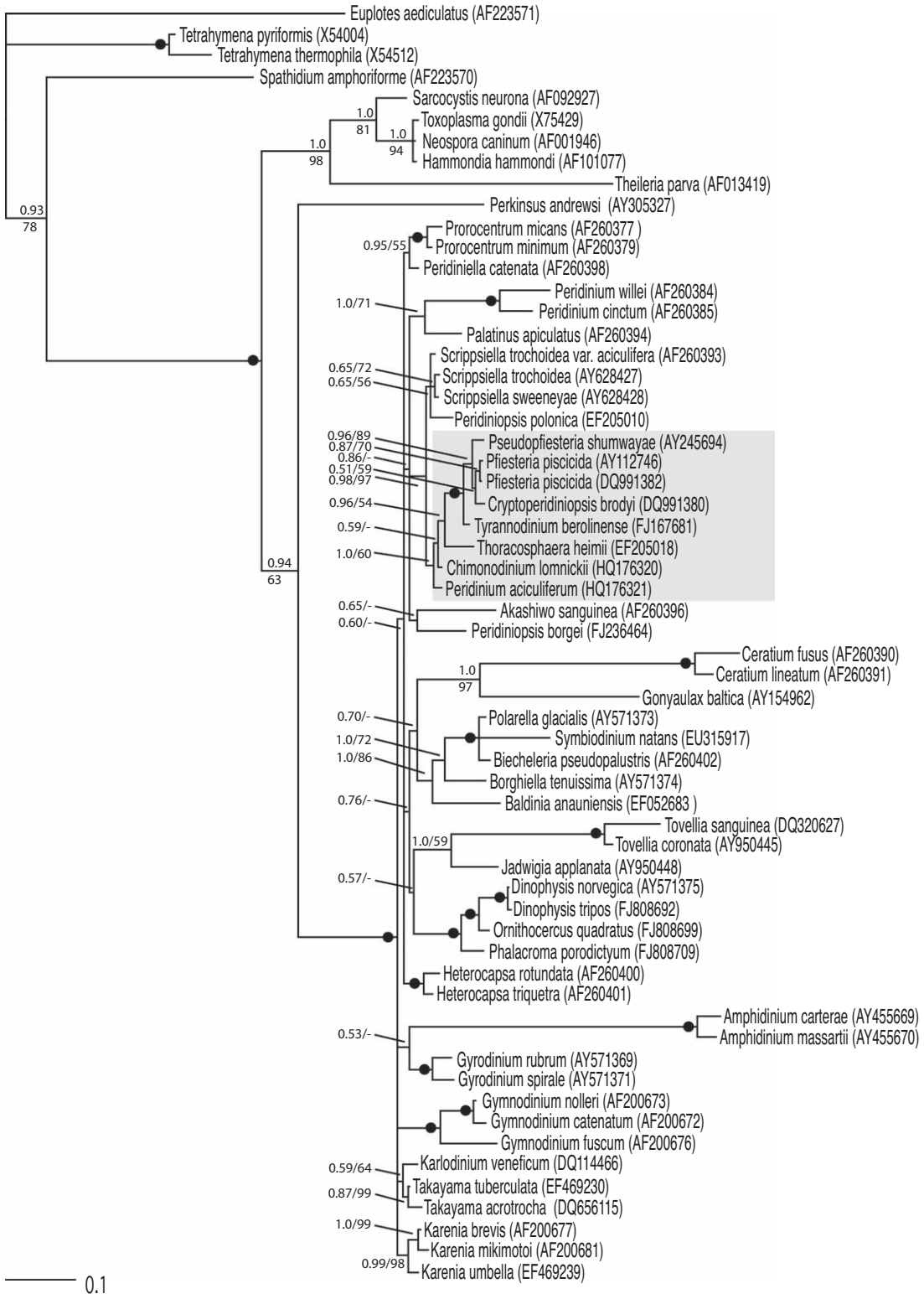

Figure 17. Phylogeny of *Chimonodinium lomnickii* and 47 other species of dinoflagellates from Bayesian inference of nuclear-encoded LSU rRNA gene sequences. The alignment included 1158 base pairs. Four ciliates, five Apicomplexa and *Perkinsus* formed the outgroup taxa. The sequence of the isolate from Greenland was 100% identical to that of the strain from Portugal and only one was used in the analysis. Branch support values

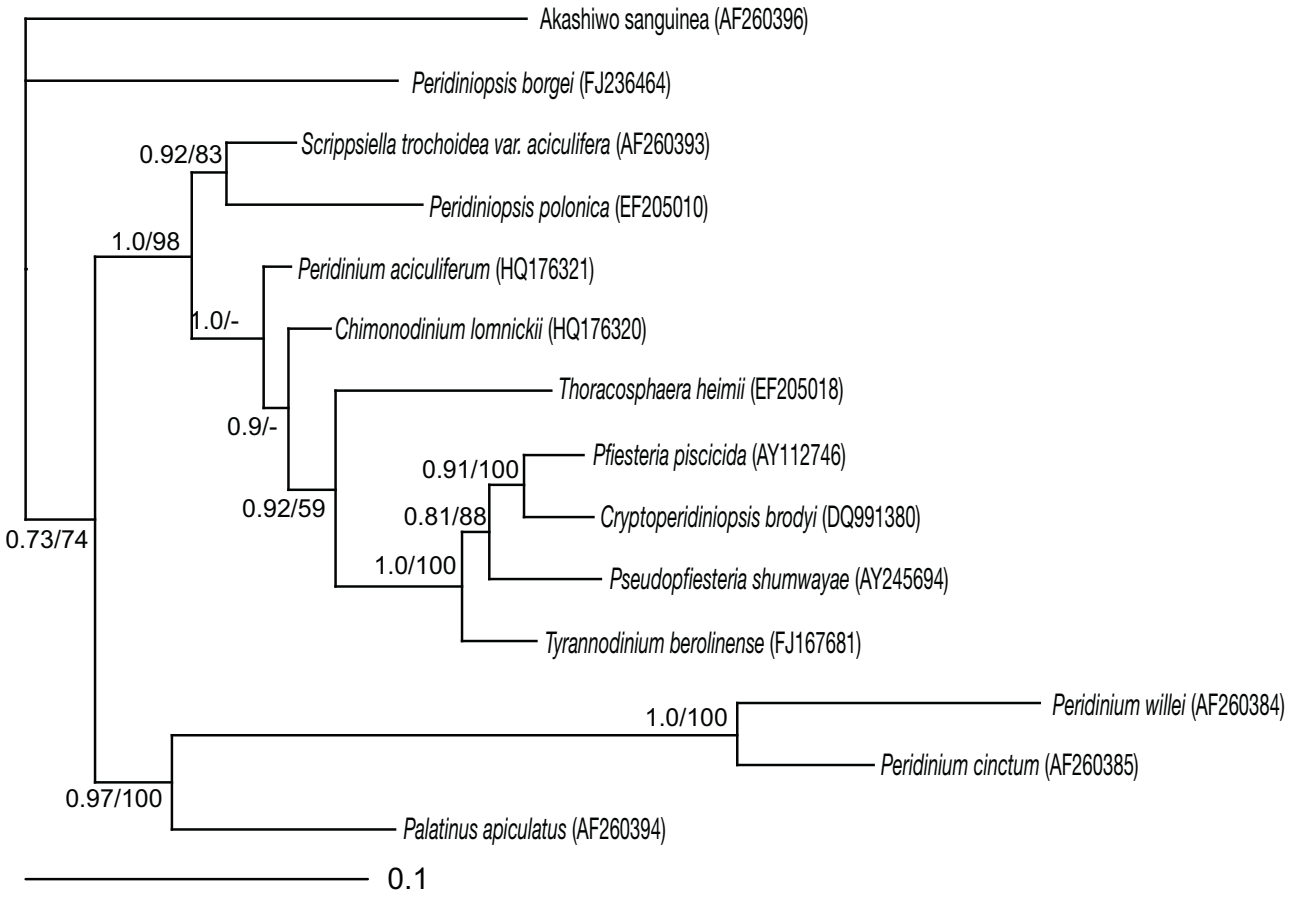

Figure 18. Unrooted phylogeny of *Chimonodinium lomnickii* and 13 closely related dinoflagellates from Bayesian inference of nuclear-encoded LSU rRNA gene sequences. The alignment comprised 1291 base pairs, including the highly divergent domain D2. Branch support values given to the left of internodes are from posterior probabilities ($\geq$ 0.5) and maximum likelihood bootstrap analyses with 1000 replications ($\geq$ 50%). Branch lengths are proportional to the number of character changes.

The presence or absence of an apical pore complex has long been the basis of the major subdivision of *Peridinium* sensu lato (Lefèvre 1932; Lemmermann 1910) and places *C. lomnickii* in a group apart from both *Peridinium* sensu stricto and *Palatinus*. However, Boltovskoy's (1979) suggestion that *P. bipes* F. Stein and *P. limbatum* (A. Stokes) Lemmermann, both with an apical pore, are close relatives of *Peridinium* sensu stricto received recent support by Logares et al. (2007). The classification of the apical pore of *P. bipes* in a type of its own (Toriumi and Dodge 1993) suggests the need for a detailed comparative analysis of this cell structure in peridinioids. The occurrence of an apical pore in species currently classified in *Peridiniopsis*, which have 6 plates in the cingulum (Bourrelly 1968, 1970), suggests a closer proximity to *Chimonodinium*, although they all display a smaller number of epithecal plates. The thecal plate organization of *P. borgei* is somewhat peculiar in having only three plates contacting the apical pore, which combines with unusual internal features (Calado and Moestrup 2002) to suggest that it may be phylogenetically distant from other so-

given to the left of internodes are from posterior probabilities ($\geq$ 0.5) and maximum likelihood bootstrap analyses with 500 replications ($\geq$ 50%). Maximum branch support (posterior probability = 1 and 100% in ML bootstrap) is indicated by filled black circles. Branch lengths are proportional to the number of character changes. The branch containing *Peridinium aciculiferum*, *Chimonodinium lomnickii*, *Thoracosphaera heimii* and the pfiesteriaceans is highlighted in grey.

called *Peridiniopsis*. The presence of a diatom-like endosymbiont in *Peridiniopsis penardii* (Lemmermann) Bourrelly and *P.* cf. *kevei* Grigorszky also indicates that species currently placed in *Peridiniopsis* form a heterogeneous group with uncertain affinities (Takano et al. 2008).

Additional aspects concerning the theca that separate *Chimonodinium* from *Peridinium* sensu stricto are the different ornamentation of plates, generally covered with areolate ridges in species of groups cinctum and willei, and the way the theca breaks open for cells to exit (see discussion in Craveiro et al. 2009). *Peridinium gatunense* Nygaard, apparently a close relative of *P. cinctum*, stands out as an exception because its theca opens along the anterior edge of the cingulum (Boltovskoy 1973), just as in *Chimonodinium*. Thecae of *Peridiniopsis borgei* and *Tyrannodinium berolinense* open in a similar way to *Chimonodinium*, whereas the cells of *Palatinus* species exit the theca through the antapical area (Calado et al. 2009, Craveiro et al. 2009).

The general cell structure of *Chimonodinium*, particularly the chloroplast organization, is essentially the same as in *Peridinium* sensu stricto (Calado et al. 1999, Craveiro et al. 2009) and contrasts both with the organization of *Peridiniopsis borgei*, with a large, starch-enveloped pyrenoid on the dorsal side of the cell, and of *Palatinus*, with radiating chloroplast lobes connected to a central, branching pyrenoid (Calado et Moestrup 2002; Craveiro et al. 2009).

In contrast with the numerous vesicles opening into the large sac pusules in the ventral areas of *Peridinium cinctum* and *Peridiniopsis borgei* (Calado and Moestrup 2002; Calado et al. 1999), typical pusular elements in *C. lomnickii* were restricted, at least near the flagellar canals, to well-defined, non-collapsed tubes about 190 nm wide. This type of pusule resembles the one described from *Palatinus apiculatus*, although three pusular tubes, rather than two, were found in that species (Craveiro et al. 2009).

Chimonodinium appears closer to *Peridiniopsis borgei* than to either *Peridinium* sensu stricto or *Palatinus* in having a well-developed system of microtubules associated with a peduncle (see below) and in the particular organization of the microtubular extension to flagellar root 3 (the TMRE). In *P. borgei* 23 microtubules of the TMRE reorganize from a flat strand near its nucleation site on the TMR to a cylindrical arrangement with a fibrous core that extends around the central sac pusule toward the back of the cell (Calado and Moestrup 2002). Although the association of the TMRE with fibrous material is much more poorly defined in *Chimonodinium*, it still suggests a closer relationship between the two genera than the molecular tree of Figure 17 displays. However, statistical support for the clade containing *P. borgei* is relatively low, and other molecular markers may be needed to further clarify its phylogeny.

Comparison with *Scrippsiella*

The similarity between the tabulation of *C. lomnickii* and that found in species of *Scrippsiella* makes an ultrastructural comparison desirable. The genus *Scrippsiella* was originally described by Balech (1959) and later validated in botanical nomenclature by the addition of a Latin diagnosis (Loeblich 1965). Only one species, *S. sweeneyae* (as '*sweeneyi*') was initially included and it is therefore the type of the genus. Vegetative cells of currently recognized *Scrippsiella* species resemble each other considerably and the morphology of the calcareous cysts (or sometimes the comparison of DNA sequences) is often required for reliable identification (D'Onofrio et al. 1999). No information on cysts of *S. sweeneyae* was given by Balech (1959) and the distinction from vegetative cells of *S. trochoidea* relies on subtle variations of some plates (Balech 1988, p. 159). Whether *S. trochoidea* is closely related or, as discussed by Fine and Loeblich (1976) and Janofske (2000), is identical to *S. sweeneyae*, its fine-structural characters are here taken as representative of *Scrippsiella*.

Several cytoplasmic features separate *S. trochoidea* from *C. lomnickii*. Whereas *C. lomnickii* lacks pyrenoids, starch-enveloped pyrenoids were represented in the original drawings of *S. sweeneyae* (Balech 1959) and are among the prominent features of vegetative *Scrippsiella* cells. The tubular structures, apparently continuous with thylakoids, that invade the pyrenoid matrix of *S. trochoidea* are similar to those reported from *S. minima* X. Gao et J.D. Dodge (Gao and Dodge 1991). The well-defined pusular tubes opening at the flagellar canals of *C. lomnickii* contrast with the higher number of less orderly, ramified vesicles shown here for *S. trochoidea*. The report of short and wide tubes in the pusule of *S. sweeneyae* by Dodge (1972) may be related to differences in fixation or in viewing angle; the aspect illustrated (Dodge 1972, fig. 11) bears no resemblance to the pusular tubes of *C. lomnickii* and we suggest that its description as a tubular pusule with invaginations is misleading. The pusule of *S. minima* was depicted as a group of vesicles radiating from the ventral area (Gao and Dodge 1991, fig. 13).

Recent phylogenetic studies have consistently shown that *Scrippsiella* species, together with other calcareous forms, share a clade with a group of non-calcareous tube feeders, the pfiesteriaceans, which include the freshwater *Tyrannodinium* (Calado et al. 2009; Gottschling et al. 2008; Meier et al. 2007). Pfiesteriacean feeding tubes are supported by overlapping rows of microtubules that form the so-called microtubular basket (Hansen and Calado 1999). However, although a less elaborate microtubular basket was found in *C. lomnickii*, none was present in the cells of *S. trochoidea* examined. In view of the widespread occurrence in dinoflagellates of peduncle-related microtubular strands, secondary loss seems the plausible explanation for the absence of a microtubular basket or a peduncular microtubular strand in *Scrippsiella*.

The emergence of the flagella through thin canals lined by odd-looking plates, as reported here for *S. trochoidea*, is unusual and brings to mind the canal plates of *Prorocentrum* (Mohammad-Noor et al. 2007; Roberts et al. 1995b). Among thecate dinoflagellates provided with furrows, similar-looking plates have only been reported from *Bysmatrum arenicola* T. Horiguchi et Pienaar (Horiguchi and Pienaar 1988, as "Scrippsiella arenicola", nom. inval.).

The features mentioned above, together with the absence of a calcareous cyst in *C. lomnickii*, agree with the molecular phylogeny in placing *Chimonodinium* separate from *Scrippsiella* (see below).

Molecular Phylogeny versus Phenotype

The tree topologies shown in Figures 17, 18 group *Scrippsiella* species on a sister clade to the one containing both *Chimonodinium* and the pfiesteriaceans. A similar result was obtained in a phylogenetic analysis based on SSU rRNA gene sequences from a large number of species, in which *Chimonodinium* is represented under the ame *Peridinium wierzejskii* (Logares et al. 2007). On the face of the extensive physiological differences between the largely heterotrophic, predatory or parasitic pfiesteriaceans (Calado et al. 2009) and the autotrophic *Chimonodinium*, a closer relationship between these groups than between *Chimonodinium* and *Scrippsiella* is unexpected. However, two non-trivial phenotypic features support this relationship: one is the presence in *Chimonodinium* of several rows of microtubules related to the peduncle, making up a relatively small microtubular basket, whereas other photosynthetic peridinioids examined have either a single microtubular strand or none at all (Craveiro et al. 2009); the other is the connection between the edge of one sulcal plate and the middle of another, involving extra-cytoplasmic fibres. This type of plate contact was first described in *Tyrannodinium berolinense* (Calado and Moestrup 1997) and seems to be associated with the contact between the peduncle cover plate and the left side of the sulcus, presumably providing the necessary flexibility to accommodate the highly dynamic feeding tube of pfiesteriaceans (Calado et al. 2009).

The tentative position of the calcareous *Thoracosphaera* as a sister clade to the pfiesteriaceans is consistent with published results (Gottschling et al. 2005, 2008). *Thoracosphaera* is unusual in that the vegetative (dividing) stage resembles the cyst stage of dinoflagellates producing calcareous cysts (Inouye and Pienaar 1983; Tangen et al. 1982). Detailed examination of the flagellate stage of *Thoracosphaera* is needed to verify if fine-structural characters corroborate the phylogenetic position suggested by molecular phylogenies.

Although *Chimonodinium lomnickii* and *Peridinium aciculiferum* appear similar in terms of their LSU rRNA gene sequences, the molecular phylogeny (Bayesian analysis) suggests that *C. lomnickii* and *P. aciculiferum* do not form sister taxa (Figs 17, 18). Rather, *P. aciculiferum* takes a basal position topologically forming a sister taxon to a large assemblage comprising pfiesteriaceans, *Thoracosphaera* and *Chimonodinium*. *Peridinium aciculiferum* is commonly regarded as closely related to *C. lomnickii* (e.g., Popovský and Pfiester 1990) and the small sequence divergence suggests that its transfer to *Chimonodinium* would be justified. However, the preliminary observation of a complete series of sections through the well-preserved ventral area of a *P. aciculiferum* cell showed neither a microtubular basket nor the pusular system found in *C. lomnickii*, raising doubts about the relationship between the two species. Further observations, preferably complemented with the analysis of additional molecular markers, are needed to clarify the phylogenetic position of *P. aciculiferum*. Also in need of taxonomic revision, judging from the affinities displayed in the molecular tree, is *Peridiniopsis polonica*, which appears related to *Scrippsiella*, although it is not known to produce calcareous cysts.

Methods

Biological material: Populations of *Chimonodinium lomnickii* from four locations were studied: Salamandersøen, North Jutland, Denmark collected in October 1994 by the late

Tyge Christensen; Lake Helen, near Kangerlussuaq (Søndre Strømfjord), Greenland, collected in March 2001; small pond near Ugglehult, Aneboda, Sweden, collected as cysts in the sediment in October 2001; and Pateira de Fermentelos, a lake near Aveiro, Portugal, collected in February 2006. Clonal cultures of *C. lomnickii* were established from vegetative cells from the Greenland sample, and from germinating cysts isolated from the Swedish sample (the latter deposited as SCCAP K-1151). All essential features were determined or verified in the population from Portugal. The morphological identity of all populations studied was verified with SEM observations and a comparison of the LSU rRNA gene sequence was performed for all except the older sample from Salamandersøen, Denmark.

The culture of *Scrippsiella trochoidea* (KF2N16; the strain is unfortunately not available anymore) used in this work was initiated from a cyst isolated from 11-cm depth (dated 1986) in core sediment from Koljö Fjord, north of Göteborg, Sweden, collected in March 2005. The cyst germinated in TL25 culture medium.

Light microscopy: Light micrographs were taken on a Zeiss Axioskop light microscope with a Zeiss Axiocam HRc digital camera (Carl Zeiss, Oberkochen, Germany).

Scanning electron microscopy: Cultured cells of *Chimonodinium lomnickii* (from Greenland and Sweden) were fixed in 3.7% formalin neutralized by $NaHCO_3$ to pH 7.5, for at least one hour. Cells were concentrated on 5 μm pore Isopore polycarbonate membrane filters, washed for one hour in distilled water, dehydrated with a graded ethanol series and critical point dried in a Baltec CPD-030 (Balzers, Liechtenstein). The dried filters were glued onto stubs, sputter-coated with platinum-palladium and examined in a Jeol JSM-6335F (Jeol Ltd., Tokyo, Japan) scanning electron microscope. Samples from Salamandersøen, Denmark, originally fixed with Lugol's solution, and Pateira de Fermentelos, Portugal, originally fixed in 5% Formalin, were dehydrated and critical point dried as above, and examined in a Jeol JSM-5400 (Jeol Ltd., Tokyo, Japan) and a Hitachi S-4100 (Hitachi High-Technologies Corp., Tokyo, Japan), respectively.

The *Scrippsiella trochoidea* cysts were collected and micrographed in a microscope preparation, and then air dried on the removed coverslip. The coverslip was glued onto a stub, sputter-coated with platinum-palladium and examined in a Jeol JSM-5400.

Transmission electron microscopy: Two different fixation schedules were used for *Chimonodinium lomnickii*: (1) cells from the Danish field sample were fixed for 1 hour in 2% glutaraldehyde in 0.1 M Na-cacodylate buffer (pH 7.4). After centrifugation and two washes in the same buffer cells were post-fixed in buffered 0.5% osmium tetroxide overnight. Following a wash in buffer, cells were dehydrated through a graded ethanol series and propylene oxide and embedded in Spurr's resin; (2) swimming cells of *C. lomnickii* from the field sample from Portugal were picked up with a micropipette and transferred to a mixture of 1% glutaraldehyde and 0.5% osmium tetroxide (final concentrations) in 0.1 M phosphate buffer, pH 7.2, for ca. 30 minutes. After one rinse in buffer, cells were embedded in 1.5% agar and post-fixed in 0.5% osmium tetroxide overnight. The agar blocks were dehydrated through a graded ethanol series and propylene oxide and embedded in Epon. Serial sections, in both cases, were prepared with a diamond knife on a Reichert Ultracut E and an EM UC6 ultramicrotomes (Leica Microsystems, Wetzlar, Germany). Ribbons of sections were picked up with slot grids, placed on Formvar film and stained with uranyl acetate and lead citrate. Serial sections of four cells were examined with a Jeol JEM 1010 (Jeol Ltd., Tokyo, Japan) transmission electron microscope.

Swimming cells from *Scrippsiella trochoidea* culture (KF2N16) were picked up and fixed for 30 minutes in 1% glutaraldehyde and 0.5% osmium tetroxide (final concentrations) in 0.2 M cacodylate buffer, pH 7.2. After one rinse in buffer, cells were embedded in 1.5% agar, washed once in a 1:1 mixture of 0.2 M and 0.1 M cacodylate buffer and washed again in pure 0.1 M cacodylate buffer. Post-fixation was in 1% osmium tetroxide in 0.1 M cacodylate buffer for two hours. The agar blocks were dehydrated as described above and embedded in Spurr's resin. The rest of the procedure was the same as for both *Chimonodinium lomnickii* fixations.

Determination of nuclear-encoded LSU rRNA gene sequences: For this study we determined the LSU rRNA gene sequence of two thecate species of dinoflagellates (viz. *Chimonodinium lomnickii* and *Peridinium aciculiferum*). Total genomic DNA was extracted from a clonal isolate of *P. aciculiferum* originating from Lake Tovel (North Italy). For this we used the CTAB extraction methods as previously outlined in Daugbjerg et al. (2000). The LSU rDNA sequence of *C. lomnickii* was obtained from single-cell PCR of cells isolated from Pateira de Fermentelos, a shallow lake near Aveiro, Portugal. This sequence obtained was 100% identical to one from a clonal isolate of *C. lomnickii* originating from a lake near Kangerlussuaq (Greenland), and 99.9% identical to strain SCCAP K-1151, originated from Aneboda, Sweden (1 point mutation, a transition T–C, out of 1291 base pairs; Genbank accession number JF430394). Since the sequences were indistinguishable we only included one in the phylogeny. The conditions used here for setting-up and running PCR were similar to those already provided in Calado et al. (2009) and Hansen and Daugbjerg (2004).

Sequence alignment: In order to infer the phylogeny of *Chimonodinium lomnickii* and *Peridinium aciculiferum* we added their LSU rDNA sequence to an alignment comprising a diverse assemblage of other dinoflagellate species. Thus, the phylogeny is based on analysis of a total of 32 genera and 45 species of dinoflagellates. Genbank accession numbers for all taxa included are given in Figure 17. Information from the secondary structure of the mature RNA molecule sensu Lenaers et al. (1989) was incorporated in the alignment. Due to ambiguous alignment of the variable domain D2 this fragment was excluded prior to the phylogenetic analyses. The data matrix was edited manually using MacClade (ver. 4.08, Maddison and Maddison 2003) and included 1158 base pairs. An additional analysis was performed with the same methods on a data matrix containing only *Chimonodinium* and 13 of its closest relatives as suggested by the more inclusive analysis. This reduction in number of taxa allowed for the inclusion of the highly divergent domain D2 sensu Lenaers et al. (1989), bringing this second alignment to 1291 base pairs including introduced gaps, without need for the use of, e.g., G-blocks as an aid to alignment. Both alignments are available from TREEBASE at **http://purl.org/phylo/treebase/phylows/study/TB2:S11241**.

Outgroup: Numerous phylogenetic studies of eukaryotes have shown that the Apicomplexa form a sister group to the dinoflagellates and, in turn, the ciliates form a sister group to the clade comprising the former two groups (e.g. Baldauf 2008). Hence, to polarize the ingroup of dinoflagellates in the more inclusive analysis we used 4 species of ciliates, 5 species of Apicomplexa and *Perkinsus* as outgroup taxa. No outgroup was used in the more restricted analysis.

Phylogenetic analyses: Bayesian analysis (BA) was performed using MrBayes (ver. 3.1.2, Ronquist and Huelsenbeck 2003) and maximum likelihood (ML) by using PhyML (ver. 3.0, Guindon and Gascuel 2003). In BA we used $2*10^6$ generations and every 50^{th} generation a tree was sampled. BA

analyses were carried out on the freely available Bioportal (www.bioportal.uio.no). To evaluate the burn-in value we plotted the LnL values as a function of generations. The burn-in occurred after 20.050 generations, thus 401 trees were removed leaving 39600 trees for generating a 50% majority-rule consensus in PAUP* (Swofford 2003). For ML analysis we applied the parameter settings obtained from MrModeltest (ver. 2.3, Nylander 2004). PhyML was run via the online version available on the Montpellier bioinformatics platform at http://www.atgc-montpellier.fr/phyml. The robustness of the tree topologies was evaluated using bootstrapping with 500 replications, for the more inclusive one, and 1000 replications, for the one including less taxa.

Acknowledgements

SCC was supported by a Ph.D. fellowship from the financing program POCI, Portugal (SFRH/BD/16794/2004) and by a grant from the European Commission's (FP 6) Integrated Infrastructure Initiative programme SYNTHESYS (DK-TAF) during July-September 2008. ND thanks the Carlsberg Foundation for equipment grants. The *Scrippsiella trochoidea* culture was established during the project "Changes in community structure and microevolution in marine protists" and was kindly provided by Nina Lundholm and Marianne Ellegaard. Henrik Levinsen provided the sample collected in Greenland and Karin Lindberg established the culture originating from cysts collected in Sweden.

References

Baldauf S (2008) An overview of the phylogeny and diversity of eukaryotes. J Syst Evol **46**:263–273

Balech E (1959) Two new genera of dinoflagellates from California. Biol Bull **116**:195–203

Balech E (1980) On the thecal morphology of dinoflagellates with special emphasis on circular [sic] and sulcal plates. An Centro Cienc Mar Limnol Univ Nac Autón México **7**:57–67

Balech E (1988) Los dinoflagelados del Atlántico Sudoccidental. Publ Espec Inst Esp Oceanogr **1**:1–310

Bibby BT, Dodge JD (1973) The ultrastructure and cytochemistry of microbodies in dinoflagellates. Planta **112**:7–16

Bibby BT, Dodge JD (1974) The fine structure of the chloroplast nucleoid in *Scrippsiella sweeneyae* (Dinophyceae). J Ultrastruct Res **48**:153–161

Boltovskoy A (1973) Formacion del arqueopilo en tecas de dinoflagelados. Rev Esp Micropaleont **5**:81–98

Boltovskoy A (1979) Estudio comparativo de las bandas intercalares y zonas panadasuturales en los géneros de dinoflagelados *Peridinium* s.s., *Protoperidinium* y *Palaeoperidinium*. Limnobios **1**:325–332

Bourrelly P (1968) Notes sur les Péridiniens d'eau douce. Protistologica **4**:5–13

Bourrelly P (1970) Les algues d'eau douce 3: Les algues bleues et rouges, les Eugléniens, Peridiniens et Cryptomonadines. Boubée, Paris

Calado AJ, Moestrup Ø (1997) Feeding in *Peridiniopsis berolinensis* (Dinophyceae): new observations on tube feeding by an omnivorous, heterotrophic dinoflagellate. Phycologia **36**:47–59

Calado AJ, Moestrup Ø (2002) Ultrastructural study of the type species of *Peridiniopsis*, *Peridiniopsis borgei* (Dinophyceae), with special reference to the peduncle and flagellar apparatus. Phycologia **41**:567–584

Calado AJ, Craveiro SC, Moestrup Ø (1998) Taxonomy and ultrastructure of a freshwater heterotrophic *Amphidinium* (Dinophyceae) that feeds on unicellular protists. J Phycol **34**:536–554

Calado AJ, Hansen G, Moestrup Ø (1999) Architecture of the flagellar apparatus and related structures in the type species of *Peridinium*, *P. cinctum* (Dinophyceae). Eur J Phycol **34**:179–191

Calado AJ, Craveiro SC, Daugbjerg N, Moestrup Ø (2006) Ultrastructure and LSU rDNA-based phylogeny of *Esoptrodinium gemma* (Dinophyceae), with notes on feeding behavior and the description of the flagellar base area of a planozygote. J Phycol **42**:434–452

Calado AJ, Craveiro SC, Daugbjerg N, Moestrup Ø (2009) Description of *Tyrannodinium* gen. nov., a freshwater dinoflagellate closely related to the marine *Pfiesteria*-like species. J Phycol **45**:1195–1205

Craveiro SC, Calado AJ, Daugbjerg N, Moestrup Ø (2009) Ultrastructure and LSU rDNA-based revision of *Peridinium* group palatinum (Dinophyceae) with the description of *Palatinus* gen. nov. J Phycol **45**:1175–1194

Daugbjerg N, Hansen G, Larsen J, Moestrup Ø (2000) Phylogeny of some of the major genera of dinoflagellates based on ultrastructure and partial LSU rDNA sequence data, including the erection of three new genera of naked dinoflagellates. Phycologia **39**:302–317

Dodge JD (1972) The ultrastructure of the dinoflagellate pusule: A unique osmo-regulatory organelle. Protoplasma **75**:285–302

D'Onofrio G, Marino D, Bianco L, Busico E, Montresor M (1999) Toward an assessment on the taxonomy of dinoflagellates that produce calcareous cysts (Calciodinelloideae, Dinophyceae): a morphological and molecular approach. J Phycol **35**:1063–1078

Eddy S (1930) The fresh-water armored or thecate dinoflagellates. Trans Am Microsc Soc **49**:277–321

Fine KE, Loeblich III AR (1976) Similarity of the dinoflagellates *Peridinium trochoideum*, *P. faeroense* and *Scrippsiella sweeneyae* as determined by chromosome numbers, cell division studies and scanning electron microscopy. Proc Biol Soc Wash **89**:275–288

Gao X, Dodge JD (1991) The taxonomy and ultrastructure of a marine dinoflagellate, *Scrippsiella minima* sp. nov. Br Phycol J **26**:21–31

Gao X, Dodge JD, Lewis J (1989) An ultrastructural study of planozygotes and encystment of a marine dinoflagellate, *Scrippsiella* sp. Br Phycol J **24**:153–165

Gottschling M, Keupp H, Plötner J, Knop R, Willems H, Kirsch M (2005) Phylogeny of calcareous dinoflagellates as inferred from ITS and ribosomal sequence data. Mol Phylogenet Evol **36**:444–455

Gottschling M, Renner SS, Meier KJS, Willems H, Keupp H (2008) Timing deep divergence events in calcareous dinoflagellates. J Phycol **44**:429–438

Grigorszky I, Krienitz L, Padisák J, Botics G, Vasas G (2003a) Redefinition of *Peridinium lomnickii* Woloszynska (Dinophyta) by scanning electron microscopical survey. Hydrobiologia **502**:349–355

Grigorszky I, Borics G, Padisák J, Tótmérész B, Vasas G, Nagy S, Borbély G (2003b) Factors controlling the occurrence of Dinophyta species in Hungary. Hydrobiologia **506–509**:203–207

Guindon S, Gascuel O (2003) A simple, fast, and accurate algorithm to estimate large phylogenies by maximum likelihood. Syst Biol **52**:696–704

Hansen G, Daugbjerg N (2004) Ultrastructure of *Gyrodinium spirale*, the type species of *Gyrodinium* (Dinophyceae), including a phylogeny of *G. dominans*, *G. rubrum* and *G. spirale* deduced from partial LSU rDNA sequences. Protist **155**:271–294

Hansen G, Moestrup Ø, Roberts KR (1996) Fine structural observations on *Gonyaulax spinifera* (Dinophyceae), with special emphasis on the flagellar apparatus. Phycologia **35**:354–366

Hansen PJ, Calado AJ (1999) Phagotrophic mechanisms and prey selection in free-living dinoflagellates. J Eukaryot Microbiol **46**:382–389

Horiguchi T, Pienaar RN (1988) Ultrastructure of a new sand-dwelling dinoflagellate, *Scrippsiella arenicola* sp. nov. J Phycol **24**:426–438

Huber-Pestalozzi G. (1950) Cryptophyceen, Chloromonadinen, Peridineen. In Thienemann A (ed.) Die Binnengewässer vol. 16, Das Phytoplankton des Süsswassers. Systematik und Biologie, part 3. Schweizerbart'sche Verlagsbuchhandlung, Stuttgart, Germany, 310 pp

Indelicato SR, Loeblich III AR (1986) A revision of the marine peridinioid genera (Pyrrhophyta) utilizing hypothecal-cingular plate relationship as a taxonomic guideline. Jap J Phycol **34**:153–162

Inouye I, Pienaar RN (1983) Observations on the life cycle and microanatomy of *Thoracosphaera heimii* (Dinophyceae) with special reference to its systematic position. S Afr J Bot **2**: 63–75

Janofske D (2000) *Scrippsiella trochoidea* and *Scrippsiella regalis*, nov. comb. (Peridiniales, Dinophyceae): a comparison. J Phycol **36**:178–189

Kalley JP, Bisalputra T (1971) *Peridinium trochoideum*: the fine structure of the thecal plates and associated membranes. J Ultrastruct Res **37**:521–531

Lefèvre M (1932) Monographie des espèces d'eau douce du genre *Peridinium*. Arch Bot **2**, Mémoire 5: 1–210, pl 1–6

Lemmermann E (1910) Kryptogamenflora der Mark Brandenburg. Bd. **3**. Algen I (Schizophyceen, Flagellaten, Peridineen). Gebrüder Borntraeger, Leipzig

Lenaers G, Maroteaux L, Michot B, Herzog M (1989) Dinoflagellates in evolution. A molecular phylogenetic analysis of large subunit ribosomal RNA. J Mol Evol **29**:40–51

Lewis JM, Dodge JD (2002) Phyllum Pyrrophyta (Dinoflagellates). In John DM, Whitton BA, Brook AJ (eds) The Freshwater Algal Flora of the British Isles. Cambridge University Press, Cambridge, pp 186–207

Lindberg K, Moestrup Ø, Daugbjerg N (2005) Studies on woloszynskioid dinoflagellates I: *Woloszynskia coronata* re-examined using light and electron microscopy and partial LSU rDNA sequences, with description of *Tovellia* gen. nov. and *Jadwigia* gen. nov. (Tovelliaceae fam. nov.). Phycologia **44**:416–440

Lindemann E (1920) Untersuchungen über Süßwasserperidineen und ihre Variationsformen II. Arch Naturg, section A **84**:121–194

Lindemann E (1924) Neue oder wenig bekannte Protisten. X. Neue oder wenig bekannte Flagellaten. IX. Mitteilungen über nicht genügend bekannte Peridineen. Arch Protistenkd **47**:431–439, pl 21

Lindemann E (1925) III. Klasse: Dinoflagellatae (Peridineae). In Schoenichen, W. (ed.) [Eyferth's] Einfachste Lebensformen des Tier- und Pflanzenreiches, 5th ed., **1**. Spaltpflanzen, Geißellinge, Algen, Pilze. Bermühler, Berlin, pp 144–195

Lindemann E (1928) Vorläufige Mitteilung. Arch Protistenkd **63**:259–260

Ling HU, Croome RL, Tyler PA (1989) Freshwater dinoflagellates of Tasmania, a survey of taxonomy and distribution. Br Phycol J **24**:111–129

Liu G-X, Hu S, Chu G-Q, Hu Z-Y (2008) Study on freshwater genus *Peridinium* (Dinophyta) from China. J Syst Evol **46**:754–771

Loeblich III AR (1965) Dinoflagellate nomenclature. Taxon **14**:15–18

Logares R, Shalchian-Tabrizi K, Boltovskoy A, Rengefors K (2007) Extensive dinoflagellate phylogenies indicate infrequent marine-freshwater transitions. Mol Phylogenet Evol **45**:887–903

Maddison DR, Maddison WP (2003) MacClade 4. Sinauer Associates, Inc. Publishers, Sunderland, Massachusetts, USA

Meier KJS, Young JR, Kirsch M, Feist-Burkhardt S (2007) Evolution of different life-cycle strategies in oceanic calcareous dinoflagellates. Eur J Phycol **42**:81–89

Moestrup Ø (2000) The Flagellate Cytoskeleton. Introduction of a General Terminology for Microtubular Flagellar Roots in Protists. In Leadbeater BSC, Green JC (eds) The Flagellates. Unity, Diversity and Evolution. Taylor & Francis, New York, pp 69–94.(Systematics Association Special Volume No. 59)

Moestrup Ø, Daugbjerg N (2007) On Dinoflagellate Phylogeny and Classification. In Brodie J and Lewis J (eds) Unravelling the Algae, the Past, Present, and Future of Algal Systematics. CRC Press, Boca Raton, pp 215–230.(Systematics Association Special Volume No. 75)

Mohammad-Noor N, Moestrup Ø, Daugbjerg N (2007) Light, electron microscopy and DNA sequences of the dinoflagellate *Prorocentrum concavum* (syn. *P. arabianum*) with special emphasis on the periflagellar area. Phycologia **46**: 549–564

Nylander JAA (2004) MrModeltest v2. Program distributed by the author. Evolutionary Biology Centre, Uppsala University

Popovský J, Pfiester LA (1990) Dinophyceae (Dinoflagellida). In: Ettl H, Gerloff J, Heynig H, Mollenhauer D (eds) Süßwasserflora von Mitteleuropa **6**. Gustav Fischer, Jena,

Roberts KR, Hansen G, Taylor FJR (1995a) General ultrastructure and flagellar apparatus architecture of *Woloszynskia limnetica* (Dinophyceae). J Phycol **31**:948–957

Roberts KR, Heimann K, Wetherbee R (1995b) The flagellar apparatus and canal structure in *Prorocentrum micans* (Dinophyceae). Phycologia **34**:313–322

Roberts KR, Timpano P, Montegut AE (1987) The apical pore fibrous complex: a new cytological feature of some dinoflagellates. Protoplasma **137**:65–69

Ronquist F, Huelsenbeck JP (2003) MRBAYES 3: Bayesian phylogenetic inference under mixed models. Bioinformatics **19**:1572–1574

Schiller J (1935) Dinoflagellatae (Peridineae) in monographischer Behandlung. In Kolkwitz R (ed.) Rabenhorst's Kryptogamen-flora von Deutschland, Österreich und der Schweiz, 2nd ed., **10** (3), Part 2 (Lief. 2), pp 161–320. Akademische Verlagsgesellschaft, Leipzig

Senzaki S, Horiguchi T (1994) A taxonomic survey of freshwater dinoflagellates of Nagano prefecture, Japan. Jpn J Phycol **42**:29–42

Starmach K (1974) Cryptophyceae, Dinophyceae, Raphidophyceae. In Starmach K, Siemińska J (eds) Flora Słodkowodna Polski 4. Państwowe Wydawnictwo Naukowe, Warszawa, Kraków, pp 1–520

Swofford DL (2003) PAUP* Phylogenetic Analysis Using Parsimony (*and other methods). Version 4. Sinauer Associates, Sunderland, Massachusetts

Takano Y, Hansen G, Fujita D, Horiguchi T (2008) Serial replacement of diatom endosymbionts in two freshwater dinoflagellates, *Peridiniopsis* spp. (Peridiniales, Dinophyceae). Phycologia **47**:41–53

Tangen K, Brand LE, Balckwelder PL, Guillard RRL (1982) *Thoracosphaera heimii* (Lohmann) Kamptner is a dinophyte: observations on its morphology and life cycle. Mar Micropaleontol **7**:193–212

Thomasson K (1963) Araucanian Lakes. Plankton studies in North Patagonia, with notes on terrestrial vegetation. Acta Phytogeogr Suec **47**:1–139

Toriumi S, Dodge JD (1993) Thecal apex structure in the Peridiniaceae (Dinophyceae). Eur J Phycol **28**:39–45

Wedemayer GJ, Wilcox LW (1984) The ultrastructure of the freshwater colorless dinoflagellate *Peridiniopsis berolinense* (Lemm.) Bourrelly. J Protozool **31**:444–453

Wołoszyńska J (1916) Polnische Süßwasser-Peridineen. Bull Int Acad Sci Cracovie, Cl Sci Math Nat, sér B **1915(8–10)**:260–285, pl 10–14

Wołoszyńska J (1936) Die Algen der Tatraseen und Tümpel. III. Peridineen im Winterplankton einiger Tatraseen. Arch Hydrobiol i Ryb **10**:188–196, 1 pl